MULTIPHASE GAS MECHANISMS

IN GROUNDWATER

By

ROBERT J. AGNEW

Bachelor of Science in Engineering Technology –
Fire Protection and Safety Technology
Oklahoma State University
Stillwater, OK
1999

Master of Science in Industrial Hygiene
University of Oklahoma Health Sciences Center
Oklahoma City, OK
2002

Submitted to the Faculty of the
Graduate College of the
Oklahoma State University
in partial fulfillment of
the requirements for
the Degree of
DOCTOR OF PHILOSOPHY
May, 2019

MULTIPHASE GAS MECHANISMS

IN GROUNDWATER

Dissertation Approved:

Dr. Todd Halihan
Dissertation Adviser

Dr. Javier Vilcaez

Dr. Greg Wilber

Dr. Lantz Holtzhower

ACKNOWLEDGEMENTS

My deepest appreciation goes to my wife, Gina, for all of her love, support, kindness, and patience throughout this arduous journey. Without her support, unending encouragement, and Pauline wisdom, I could not have finished this task. Her steadfast love has been a buttress against the pressure of this labor and has maintained some semblance of normalcy in our lives, allowing our children to grow and prosper. My children, Caelyn, Xander, and Rowan also have my thanks and admiration for enduring the long hours with me away from home, the missed games, and missed performances.

The illustrations in this work are by Liz Roth, Professor of Painting and Drawing, Department of Art, Graphic Design and Art History, Oklahoma State University and by Veronica Reed. This work would be all the poorer without your artistic abilities.

This study was made possible by the generosity of the Bruno family who has made the Arbuckle-Simpson Ranch available for various research projects. The Nature Conservancy has facilitated the research at the Arbuckle-Simpson Ranch and has provided lodging at the Pontotoc Ridge Preserve. A special thanks to Jona Tucker for generous support of this project in providing logistics and helping hands of her team, including Andrew (Andy) Schofield, Justin Anderson, and Taylor McNutt. The authors are grateful to Andrew Hunt and the USGS for conducting the whole gas analysis. Additional thanks to Dwain Airhart and Nick Johnson, OSU graduate students for

helping with the weir installation. Thanks to Veronica Reed for proofreading and editing this manuscript.

Thank you to my committee. Your guidance and support have enabled me to grow as a scientist and a researcher. I appreciate all of your support, wisdom, and insight. Finally, last but certainly not least, my heartfelt thanks go to my adviser Todd Halihan. Your wit, humor, and knowledge have been well appreciated. I very much enjoyed our discussion sessions and time in the field.

Name: ROBERT J. AGNEW

Date of Degree: May, 2019

Title of Study: MULTIPHASE GAS MECHANISMS IN GROUNDWATER

Major Field: ENVIRONMENTAL SCIENCE

Abstract: Numerous groundwater springs bubble, yet the flow and transport of gases are not well understood in hydrogeology. An understanding of the processes by which gases enter, migrate, and are liberated from groundwater is required. A quantitative conceptual model of gas migration in groundwater will allow an understanding of what informative aquifer signals may be present in gas data, as well as what information signals may be masked or diminished by phase changes. Through analysis of existing published literature, seven facies of groundwater bubbles were developed to provide a framework for research in these specific categories of gas transport. In order to better understand these multiphase bubbling springs, an instrument was designed and deployed over the discharge of a spring in southern Oklahoma that measured the total gas flux, ebullative and diffusive. By measuring the water discharge from the spring too, a hydropneumograph of gas and water mass flux over time can be produced. In addition to the mass flow rates of the two phases provided by the hydropneumograph, water and gas samples were collected for compositional analysis. By combining the compositional data of exsolved and dissolved gas with the mass flow rates from the hydropneumograph, estimation of the quantity of light noble gases is radically changed (60% for He, 45% for Ne) which provides improvements in the calculation of recharge temperature of 4 to 25% depending on the model selected. These improvements in the understanding of the physical hydrogeology of bubbling springs provide an additional avenue for researchers to explore aquifer dynamics that is largely ignored in the extant literature.

TABLE OF CONTENTS

Chapter Page

LIST OF TABLES

LIST OF FIGURES

Figure Page

CHAPTER I

INTRODUCTION

Motivation

The mechanisms leading to the formation of bubbles in springs and wells have received minimal attention beyond composition and causation. Free phase gas transport quantification provides insight into a range of topics, from hazards that need to be managed, prediction of earthquakes, to the economic value of soda waters. The presence of free-phase gas or vapor bubbles in groundwater provides valuable information about the subsurface flow system. Additionally, free-phase gas or vapor bubbles may strip dissolved gasses from solution and introduce error into the assessment of gas composition in springs. These errors affect analyses such as recharge temperature and groundwater apparent age, thereby altering results related to paleoclimate and global climate change. Finally, an understanding of the free gas phase in groundwaters may provide insight into water quality and improve drinking water supply management.

Current Science

The presence of bubbles in groundwater has a long history in scientific commentary, dating back to at least 15 B.C.E with Vitruvius (Pollio/Rowland c. 15

B.C.E/1999). Darcy credits Vitruvius with providing the early understanding of springs (Darcy/Bobeck 1856/2004), though his work does not include free phase gas. Meinzer's (1927) classification of springs by discharge rate provides an early contemporary source for understanding springs in the United States. Following Meinzer's system of classification, bubbling springs may be classified by type, or facies.

Descriptions of bubbling springs are sparse, but sufficient literature exists to classify distinct facies. Organizing the facies by the depth below the surface where the gas process occurs provides structure for the classification system. Starting with near-surface phenomenon, biological processes from microbes generate the gas for Type I bubbles with early work by Blesson (1832) related to the ignition of swamp gasses and later quantification of the gas species responsible for spontaneous ignition by Comas et al. (2008).

Two types of bubbling springs occur in shallow aquifers, most typically in karstic aquifers, from the entrainment of air, Type II, and the degassing of water through velocity effects, Type III. Air entrainment was first postulated as a syphon effect by Gavrilović (1967) while observing bubbles turning on and off in a karstic spring. Type III degassing springs, which are not effervescent, are sparsely described in groundwater literature (Thomas et al. (2002). However, the phenomena is described in water treatment literature (Scardina, 2004) (Scardina & Edwards, 2006) and is caused by a velocity induced pressure drop, following Bernoulli's principle, and degassing slightly over saturated gas from water.

Soda springs, Type IV, represent the most classic type of bubbling springs. Soda springs have received much attention from the early works of Anderson (1890) regarding

trace minerals and economic vitality of mineral waters. Recent works (Lewicki, et al., 2013) explore the importance of soda springs in the global carbon cycle and global climate change, including sequestration of carbon dioxide in deep aquifers. These springs bubble due to the dissolution of carbonates at depth resulting in several atmospheres of excess pressure, which manifests as the familiar effervescence of soda water.

Waters that encounter petroleum deposits may uptake flammable gasses and transport them to the surface where bituminous bubbles may evolve and pose a health and fire risk. These flammable bubbles provided an early method for the location of carboniferous formations, including coal deposits. Presently, the evolution of Type V bubbles, and the study of their composition (methane and hydrogen sulfide), is providing insight into sub-surface lithologies and processes in Greece (Etiope, et al., 2006) (Etiope, et al., 2013).

The last two deep facies have either direct (Type VI) or indirect (Type VII) contact with gases from depths reaching the mantle. Type VI bubbles are water vapor from the result of groundwater in contact with sufficient heat from a geothermal source to boil at or near the surface, as present in the Yellowstone Heart Lake Geyser Basin (Lowenstern, Bergfeld, Evans, & Hurwitz, 2012). Type VI bubbles may also contain mantle derived gasses typical of Type VIII mantle bubbles, the boiling action overwhelms the physical detection of mantle bubbles and only chemical analysis would reveal the mantle-gas connection. Mantle bubbles are the most well represented facies in the literature from a compositional perspective with significant work provided by Mazor & Wasserburg (1965) and Bräuer et al. (2013) related to the determination of gasses from the mantle.

In addition to the hydrogologic literature, albeit sparse, on the types and abundance of free-phase gasses in groundwaters, the geochemical literature on the dissolved gas phase in natural waters is abundant. The solubility of noble gasses in natural waters is dependent upon the temperature and pressure of equilibration and the solubility of each noble gas varies according to temperature (Weiss R. F., 1970) (Weiss R. F., 1971) (Weiss & Kyser, 1978) (Clever, 1979).

The solubility of noble gasses in natural waters as determined by Weiss and by Clever applied only to air-equilibrated water (rain, lakes, etc.). Analysis of dissolved noble gasses in groundwater shows that the quantity of gas in groundwater far exceeds that of air-equilibrated water. Heaton and Vogel (1981) coined the additional quantity of dissolved gas as "Excess Air" and provided a model for its formation related to bubble entrapment in the soil matrix below the surface of the groundwater and the subsequent equilibration at higher pressure.

By using the relationship of temperature and solubility and continuing the work of Andrews and Lee (1979) and Heaton and Vogel (1981) on excess air, Stute & Schlosser (1993) developed a paleothermometer that on combination with their groundwater dating technique (Schlosser, Stute, Sonntag, & Münnich, 1989) allowed the determination of the recharge temperature and age of groundwaters emerging at springs. This technique led to improved estimations of the cooling of tropical Brazil (5˚C) during the last glacial maximum (Stute, et al., 1995) and established the science of climate reconstruction using groundwater data. The modeling of paleotemperature was then later refined by Aeschbach-Hertig et al. (2000) into the form widely used today.

Dissolved gas content has shown to be valuable in the determination of groundwater apparent age and recharge temperature. However, the extant literature on groundwater temperature and age reconstruction is void of discussion of bubbles at the discharge sites where the water samples are collected. Literature in both the hydrogeologic and chemical engineering fields (White, Hem, & Waring, 1963); (Baird, Bottomley, & Taitz, 1979); (Patoczka & Wilson, 1984); (Lucchetti & Gray, 1988); (Vroblesky & Lorah, 1991) (Mariner, Evans, Presser, & White, 2003) (Daniel, 2018) acknowledge the effects of bubbles on dissolved gas content. Dissolved gases will migrate into bubbles based upon the gas species' Henry's Air-Water Partitioning Coefficient (K_{aw}) and their diffusivities (Holocher, et al., 2002).

Objective and Relevance of the Research

Based upon the understanding of the physical mechanisms of bubble-facilitated transport, the abundance of bubbling springs, and the omission of observations of bubbles in pertinent temperature and age reconstruction research, there is a clear need to quantify the errors related to the estimation of these parameters in bubbling springs. By quantifying the errors in parameter estimation through physical measurement, the assumptions about the error based on the governing theoretical principles may be tested. In doing so, existing data may be re-evaluated in light of the possible errors and updates may be made to existing recharge temperature and age data. Additionally, these error estimates will provide future researchers with a basis for determining when the quantification of the free gas phase at a bubbling spring may be necessary to achieve the desired accuracy of parameter estimates.

Research Design

In order to enable greater accuracy in the determination of the mass discharge of gas and water-gas ratios (WGR) in groundwater from springs, a field-deployable instrument using commercially available components has been developed to independently measure the gas and water mass flow rates in springs with bubbling mixed-phase flow. By installing a phase separator at the spring discharge, a thermal mass flow sensor is utilized to measure the gas flow rate (ebullition + diffusive flux) generated from a spring. The water flow rate is determined by a standard weir. Field performance of the device was tested on a spring discharging from the Arbuckle-Simpson aquifer near the town of Connerville in south-central Oklahoma, USA.

Dissolved gas data were determined by water and free gas sampling and analysis by mass spectroscopy. Compositional results are combined with physical measurements to determine accurate gas concentrations than are then used in computational modeling of recharge temperature and apparent age. The modeling results are compared between water only and water+gas results to quantify errors associated with the omission of the free gas phase.

Dissertation Organization

This work begins with a broad review of the existing literature that discusses the presence and types of bubbles in groundwater. Through this review, seven bubble facies (or types) are defined. These facies allow for a chemical and mechanistic understanding of the various ways groundwater may become gassy, how the dissolved and free gas is transported in aquifers, and the mechanisms for the evolution of bubbles at the discharge

point. At present, several terms related to gas in groundwater are used either informally, interchangeable, or both. In order to facilitate the scientific discussion of gas/water phenomenon, specific terms are defined and summarized in a glossary.

Discussed in the methods chapter is the measurement of the free gas phase discharge from bubbling springs. Outside of some commercially viable soda springs, quantification of the gas flux, or volumetric flow, from bubbling springs is virtually absent in the scientific literature. Described in this work is an instrument for capturing the ebullitive (bubbling) and diffusive gas flux at a spring discharge, combined with a standard weir to measure the flow of the discharging water of a bubbling spring in south-central Oklahoma. The resulting two flow rates are plotted versus time to create a hydropneumograph. The hydropneumograph provides a new tool for the understanding of aquifer dynamics.

The fourth chapter combines the bulk gas and liquid flow data with dissolved and free gas chemical analysis to provide a total gas composition of the waters of the aquifer. This analysis provides two data sets, dissolved gas and dissolved+free gas, for use in the determination of recharge temperature and apparent age through modeling software. By comparing the dissolved gas to the dissolved+free gas content, and estimation may be made for the error in ignoring free gas when computing recharge temperature and apparent age. This work shows that error is in fact introduced into the estimation of recharge parameters (age and temperature) if the free gas phase is ignored in ebullating springs. The error in the estimation of excess air leads to a modest error in predicted Nobel Gas Temperature (NGT) of nearly 2%, proportional to the difference in the He/Ne ratio. The difference between the errors of He and Ne quantity are proportional to the

difference in dimensionless Henry's Air-Water partitioning coefficient (K_{AW}) in He and Ne and therefore drive a proportional error in the estimation of apparent age.

Finally, in the concluding portion of this work, the implications of the results are provided along with potential future work that is a natural extension of the findings. First, the error associated with the estimation of recharge temperature and age has implications for the field of paleotemperature reconstruction and subsequent modeling of earth climate and understanding of global climate change. Second, the hydropneumograph demonstrated that the free phase gas generation rate may increase prior to a corresponding increase in groundwater flow. This phenomena may be useful in predicting changes in groundwater quality. For large springs that are used as a drinking water supply, and that may be susceptible to a decrease in water quality from surface water incursion during storm events, an increase in gas flow may be an a priori indicator of diminished water quality and allow for intervention.

CHAPTER II

LITERATURE REVIEW

Why Springs Bubble: A Framework for Gas Discharge in Groundwater

Article Publication: Published in Groundwater (Agnew & Halihan, 2018), used here in accordance with the Wiley Publishing Services Copyright Transfer Agreement – Permitted Uses By Contributor.

Authors: Robert J. Agnew and Todd Halihan

Two important questions when evaluating the discharge of gas in groundwater include, “Are free phase gasses significant?” and “What does free gas tell us about the groundwater system?” A classification system for gas discharge in groundwater fosters a better understanding of bubble and spring dynamics. For example, an oil seep, a water spring, and a volcano are all liquids discharging at the surface, but they are not the same. The differences in bubbles issuing forth from groundwater provide a valuable dataset for the evaluation of groundwater flow. By providing a classification system for gasses emanating from groundwater, several benefits emerge for the research community

including, better utilization of gas phase data for economics or hazard evaluation, interpretation of groundwater flow paths, and a consistent set of terminology for developing research questions.

The economic impact of free phase gases in groundwater provides both profits and losses. Sparkling water sales in 2016 for just the United States, amongst the top five brands, totaled $1.3 billion (Statista 2016). Maintaining the gas phase chemistry of the sources of these fluids is just as important as the fluid phase chemistry for this use; Perrier collects water and carbon dioxide separately and combines them during bottling for product consistency (Nestlé 2016). The mixed phases of oil and gas in petroleum exploration are a significant economic challenge for producers as the bubbling of gas from the crude may take an extended period and may damage pumps if not separated properly (Lavenson, et al. 2016). For CO_2 sequestration, loss of CO_2 from disposal zones coming back to the surface determines the long-term effectiveness of the technique. Shipton et al. (2005) examined bubbling CO_2 in Paradox Basin, UT as a proxy for potential leakage. For tertiary hydrocarbon production, loss of CO_2 is actually costly for production budgets and these systems consider storage as a loss.

Gas discharges may also pose health and environmental risks. In 1986 the soda spring fed (Clarke 2001) Lake Nyos, Cameroon underwent massive exsolution of CO_2, engulfing the nearby villages in a blanket of CO_2 gas and killing an estimated 1,250 people (Freeth 1992; Clarke 2001). Additional lakes in the region, including Lake Monoun, have similar gas saturation build-up and present a risk to public safety. Through intervention, engineered systems have reduced the risk level using controlled degassing techniques (Kusakabe et al. 2008).

Methane discharging in springs is common due to hydrocarbon deposits or near-surface methanogenesis frequently occurring with groundwater. Discharging flammable gas may lead to a deflagration risk if the concentration is sufficient. Flammable gas discharge at springs and swamps may contain trace gases that increase the likelihood of spontaneous ignition. The Rev. John Mitchell (1829) provided an early hypothesis of the substance responsible for the *Ignis Fatuus*, phosphuretted hydrogen i.e. phosphine, PH_3. Mills in, *Will-o'-the-wisp revisited* (2000), provides an additional hypothesis on the spontaneous ignition of methane with variants of phosphine. Mills comments that legends of Will-o'-the-Wisps killing wayward travelers originate because phosphine is deadly at the low concentration of 0.5 mg/l. S. Morgenstern (1973) colorfully describes the legends of the deadly phenomenon of the *Ignis Fatuus* as a "Fire Swamp," referring to the location in Guilder.

Bubbles can also facilitate contaminant transport and may appear in and around spring discharges from the natural decay of surface organic matter. Vroblesky and Lorah (1991) describe the decomposition of organic sediment in a creek in Maryland producing methane from anaerobic decomposition and the presence of chlorinated volatile organic compounds (VOCs) in the free gas phase. The methane production in the creek was acting to strip VOCs from the contaminated groundwater. Methane production can induce ebullition-facilitated transport of tar deposits from contaminated sediments to the surface of the water (McLinn and Stolzenburg 2009). Tar in the river sediment is not particularly harmful, but when transported to the surface of the water it travels to the shoreline and creates a nuisance for beachgoers.

The presence and composition of free phase gas discharging from aquifers are valuable data for investigating aquifer characteristics, even though White et al. (1963) concluded that a free phase gas is uncommon. A good example of the usefulness of free phase gas data is the work of Sugisaki and Sugiura (1986) who noted evidence of gas anomalies in He/Ar, N_2/Ar, and CH_4/Ar ratios at mineral springs before earthquakes. Additionally, the gas-water ratio in a bubbling spring can estimate the water flow rate in the aquifer (Taran 2005). The presence of bubbles may also act to mask information if not properly considered. Failing to account for the free gas phase may introduce significant errors in determining the total gas present if only the dissolved phase is analyzed. Surficial bubbles (typically biogenic in origin) may act to strip out dissolved gases, which would introduce error into a dissolved gas analysis (White et al. 1963; Baird et al. 1979; Patoczka & Wilson 1984; Lucchetti & Gray 1988; Vroblesky and Lorah 1991; Mariner et al. 2003). This work describes that bubbles may also indicate biological activity, void spaces, petroleum deposits, high groundwater velocity, mineral composition, petroleum deposits, and other geochemical and geophysical phenomena.

This work does not intend to provide an exhaustive understanding of bubble formation and the physics behind bubble nucleation, growth, detachment, and coalescence. For an in-depth review of bubble physics see Lavenson et al. (2016). The formation of bubbles at nucleation sites has been established using four mechanisms as described by Jones et al. (1999), but they are not included in this work. Finally, an understanding of gas solubility in water is derived from Henry's Law and the associated Henry's Law Constants (Henry 1803;Sander 1999). As this work is focused on free phase

gas from groundwater, this basic physics is excluded except where needed as part of the classification scheme.

The lack of proper use of technical terms in existing literature and site names contributes to the difficulty in discussing free phase gas in groundwater. The simpliest example is "boiling" spring to describe a spring with churning water at temperatures below boiling. These systems may or may not have free phase gas, but the temperature and gas condition is not clearly described. A glossary is provided in this work to clarify the terminology used for describing phase changes in hydrogeologic systems.

This framework for the classification of gases in groundwater systems proposes seven categories or facies. The proposed framework will allow a more robust use of language related to the measurement, modeling, and prediction of the flow of gases phases in groundwater. Supporting the framework is a literature review of the historical and contemporary research for each free phase gas facies (Table 2). Each section on individual facies provides examples of the type spring and implications for the aquifer. An additional section discusses factors where multiple facies may be present. The facies are categorized by the underlying phenomenon generating the free phase gas, and each facies is numbered in the order of relative depth of the underlying mechanism most commonly encountered.

Classification System for Free Phase Gas Discharge

While there are a number of frameworks to describe and categorize springs and groundwater based upon water type and origin (Bryan 1919; Meinzer 1927; Alfaro and Wallace 1994), a systematic categorization and review of the free phase gas discharge in groundwater is lacking. The categorization, naming, and description provided here uses

seven common manifestations or facies, Types I-VII, (Table 1) based upon a) how the groundwater becomes gas charged and b) how the gas comes out of solution. The categorization also considers c) gas composition and d) implications for aquifer dynamics. For consistency, a formal naming process is needed to distinguish between gases discussed informally and ones following this framework. A free phase gas discharge or bubble with a specific origin is expressed in this system by stating the facies name followed by a corresponding Roman numeral (e.g. Biogenic (I) bubbles). These facies are divided into shallow (facies I-IV) and deep (facies V-VII) origins, based on their common occurrence.

The seven facies presented in this work represent the unique sources and mechanisms of bubbles in springs described in existing peer reviewed literature. The name of each facies type corresponds to the most commonly used reference to the hydrogeologic setting or literature name. For example, Biogenic (I) discharges originate from microbial metabolic processes such as methane generated by the biotic decomposition of organic matter, typically near the surface. These may also form from methanogenesis at depth. While both cases generate methane, the key component of the facies is active biological production, not the gas itself. Biogenic methane is distinct from methane related with petroleum features, which do not involve an active biological process; these are Bituminous (V) bubbles. Carbon deposit is the determining feature of the facies, not methane; hydrogen sulfide bubbles coming from a petroleum deposit would also be Bituminous (V) bubbles.

Table 1: Bubble Facies by Relative Depth

Bubble Facies (shallow to deep)	Common Name	General Spring Type	Type Spring	Characteristic Gas(es)	Gas Source	Mechanism of dissolution	Implications for Aquifer
I	Biogenic	Bog	Caribou Bog, Maine, USA	Methane ($\delta^{13}C$ -68% to -91% w/o ethane: Modern Carbon)	Biogenic Decomposition	Gas concentration increases beyond saturation via microbial production	Generally a surface phenomenon (may strip gasses from depth)
II	Entrained Air	Karst	Kojin Spring, Serbia	Air (Nitrogen, Oxygen)	Air Entrainment	False dissolution, gas stays in gas phase	Aquifer void space
III	Bernoulli	Fracture/Karst	Byrds Mill Spring, Ada, OK	Nitrogen	Atmospheric absorption	Velocity pressure drop	Locally high velocity at the spring orifice
IV	Soda	Mineral/Soda	Perrier Spring, Vergeze, France	Carbon Dioxide	Mineral dissolution (Decarbonation of marine carbonates)	Pressure drop as water rises from depth	Underlying mineral composition, aquifer temperature
V	Bituminous	Various	Kaiafas Lake Spring, Greece	Methane ($\delta^{13}C$ -25.4% to -76% w/ ethane: Dead Carbon)	Bitumen Decomposition	Pressure drop as water rises from depth	Petroleum Reservoir connectivity
VI	Boiling	Hot Spring	Heart Lake Geyser Basin, Wyoming, USA	Water Vapor	Ground Water	Phase change of water (boiling) from pressure drop as water rises from depth + temp.	Geothermal activity
VII	Mantle Gas	Various	Eifel Volcanic Field, Germany	Helium	Mantle	Pressure drop as water rises from depth	Deep aquifer connectivity

Table 2: Bubble Facies Literature

Table 2: Bubble Facies Literature				
Bubble Facies (shallow to deep)	**Facies Number**	**Early Description of Phenomenon**	**Early Description of Facies**	**Contemporary Description of Facies**
Biogenic	I	Blesson (1811)	Mills (1829)	Comas et al. (2008)
Entrained Air	II	Gavrilović (1967)	Bonacci & Bojanić (1991)	Kansou & Bredeweg (2014)
Bernoulli	III	Bernoulli (1738)	Fairley (1881)	Krešić (2007)
Soda	IV	Henry (1803)	Anderson (1890)	Lewicki et al. 2013
Bituminous	V	Vitruvius (c. 15 BC)	Geological Society of Pennsylvania (1832)	Etiope, et al. (2006)
Boiling	VI	De Luc (1772)	LeCont (1855)	Lowenstern, et al. (2012)
Mantle	VII	Mazor-Wasserburg (1965)	Mazor & Wasserburg (1965)	Bräuer et al. (2013)

Shallow Bubble Facies

Free phase gas facies of Types I – IV, as shown in Figure 1, tend to occur in relatively shallow formations. They include Biogenic (I), Entrained Air (II), Bernoulli (III), and Soda (IV) bubbles. For the purposes of this categorization system, shallow refers to the aquifer being above the base of treatable fresh water.

Type I – Biogenic

Type (I) bubbles are those emanating from a microbial metabolic process producing gas, typically methane. While dissolved CO_2 may be from a presently living

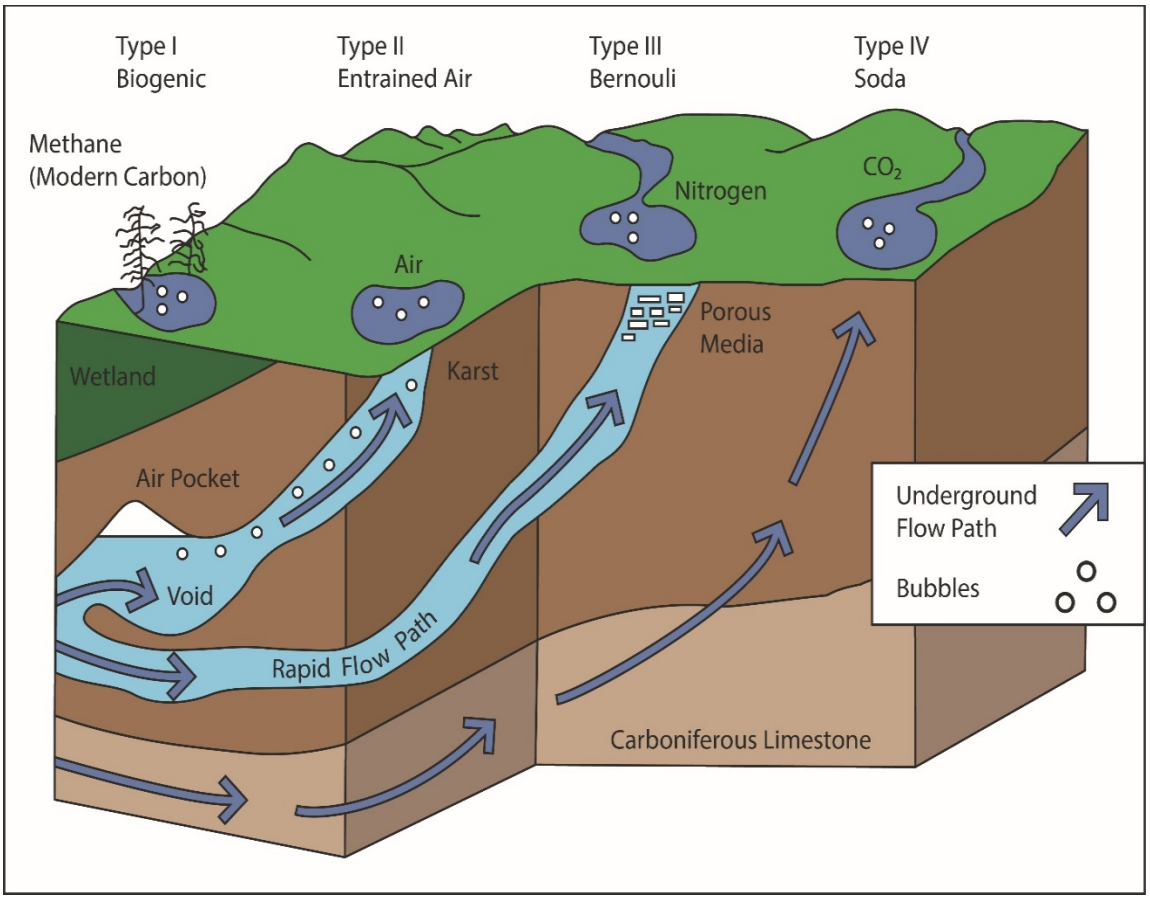

Figure 1. Bubble Facies I-IV.

biogenic source, the evolution of bubbles of methane from biogenic decomposition proves more common in groundwater. The conceptual model for the presence of Biogenic (I) bubbles in groundwater begins with an active metabolic process undertaken by living microorganisms. This is in contrast to the dissolution of deposits of formerly living marine carbonates common to Soda (IV) bubbles. Biogenic (I) bubbles may originate in the deeper sub-surface or surficially depending upon the location of microbial activity. Seeps around landfills are commonly associated with bubbling methane (Hackley and Panno 2004). Biogenic (I) bubbles are methane with a modern carbon signature (δ13C -68% to -91% without the presence of ethane) (Schoell 1980).

Major L. Blesson (1832) provided one of the earliest credible accounts of Biogenic (I) bubbles in describing the phenomenon of the *Ignis Fatuus*, or Will-with-the-Wisp/Will-o'-the-Wisp. *Ignis Fatuus* or "foolish fire" comes from English folklore and is a flame or light appearing over a swamp or bog, which may lure a traveler off the path and bring about their demise. Blesson (1832) observed the location of bubbles in a bog in Germany in 1811 and returned at night to observe the *Ignis Fatuus*, establishing the connection between the swamp bubbles and the fire like phenomenon. Mills (2000) noted reports of the *Ignis Fatuus* all but disappeared in modern times, but Żychowski (2013) reported the phenomenon of *Ignis Fatuus* over a mass grave in Niepołomice, Poland. Żychowski (2013) provides a plausible chemical reaction between groundwater, soil, bacteria, organic and mineral matter, and the atmosphere fitting the descriptions of *Ignis Fatuus,* corroborating the spontaneous ignition hypothesis.

Biogenic (I) bubbles are commonly found in peat bogs. Comas et al. (2008) discusses the biogenic gas phenomenon in peat bogs in Maine, describing the methane flux and the observation of a two-meter diameter methane bubble trapped in ice during the winter. Gas discharges from these and similar peat bogs may be of increasing interest due to their correlation with increased gas production and warming climate (Comas et al. 2008). This site would be a useful type location for the Biogenic (I) facies. Blesson (1832), Mitchell (1829), Mills (2000), and Żychowski (2013) all describe surficial Biogenic (I) bubbles, whereas Bräuer et al. (2005) describes rare Biogenic (I) bubbles from the sub-surface. Methane production on the surface and at depth is the result of metabolism of methanogens, single celled Archaea (Chapelle et al. 2002). Pedersen

(1999) and Chapelle et al. (2002) discuss a hydrogen driven deep biosphere that metabolizes mantle-derived hydrogen to produce CO_2 and methane.

Type II – Entrained Air

The conceptual model for the Entrained Air (II) facies is a siphon effect that entrains air from a cave conduit into the aquifer flow path and then emerges as bubbles in spring discharge. There is no mechanism of exsollution as the entrained air never enters the dissolved phase. Karst formations provide favorable conditions for the development of the Entrained Air (II) facies as they are recharged by surficial water containing atmospheric gas and form cavities, which may accumulate pockets of gas (Bonacci and Bojanić 1991; Panno et al. 2001).

Some rhythmic springs appear with intermittent Entrained Air (II) bubbles as described by Gavrilović (1967) in the Dinaric Karst region, notably Kojin Spring, Serbia. Additionally, May Spring in Southwestern Illinois has been documented to discharge large volumes of air (Panno et al. 1996). Modeling of the siphon effects of springs through qualitative reasoning have been conducted to quantify the effect at Fontestorbes spring (Kansou and Bredeweg 2014) but show that for this spring a simple siphon model may be incomplete.

Type III – Bernoulli

The conceptual model for the presence of Bernoulli (III) free phase gas discharge in a spring begins with air dissolving into meteoric water and then transported into an aquifer. The dissolved oxygen is consumed by subsurface reactions, largely biotic,

leaving primarily nitrogen and other atmogenic gasses in the water (Davis & DeWeist 1966) that come out of solution as bubbles due to the pressure drop at the discharge site (S. V. Panno 2001). The water in the aquifer moves relatively slowly due to the large cross-section of the aquifer. The water accelerates through converging flow lines or a small orifice or gravel bed close to or at the spring discharge, causing an increase in the velocity near the end of the flow path resulting in choked flow and a pressure drop following Bernoulli's Principle. The pressure drop results in gas coming out of solution and forming bubbles, most commonly composed of nitrogen. Bernoulli (III) bubbles follow the similar well-documented phenomenon of degassing of CO_2 and the precipitation of calcite in the formation of advancing waterfalls and / or tufa due to a change in the partial pressure of the solute due to the increased stream velocity (K. C. Hackley et al. 2007).

Bernoulli (III) free phase gas discharge arises from the phenomenon of a drop in partial pressure induced by an increase in fluid velocity (velocity pressure or kinetic hydraulic head). As the velocity pressure drops, the partial pressure of a dissolved gas can exceed the pressure of the environment and ebullate. Bernoulli's treatise *Hydrodynamica* (1738/1968) established the relationship between a moving fluid and pressure-drop, giving rise to the Bernoulli Principle and the Venturi Effect. This relationship was used by Fairley (1881), who was among the first researchers to describe "Blowing Wells," water wells that have a perceptible gas flow at the top of the bore. Fairley (1881) used Boyle's law to estimate the size of a rock cavity as a correction for degassed flow, showing a correlation with increased gas flow and decreased atmospheric pressure.

Literature from the water treatment industry illustrates how the change in the velocity pressure of the water, and therefore the partial pressure of the dissolved gas, induces a phase change and the evolution of bubbles in filter beds made of sand (Scardina 2004; Scardina & Edwards 2006). Heaton and Vogel (1981) describe water containing "Excess Air," water with a greater amount of dissolved nitrogen and argon than would be expected from atmospheric equilibrium. Additionally, Klump et al. (2008) and Solomon et al. (2011) describe the development of excess air in groundwater from the rising and falling of the water table in porous media. A mathematical model and a laboratory experiment explaining the mechanism for the development of excess air, or nitrogen, in springs was developed (McLeod et al. 2015). This facies differs from the Entrained Air (II) facies in that the gas becomes dissolved in the water, and then comes out of solution to form Bernoulli (III) bubbles.

Some of the most relevant research related to the formation of nitrogen bubbles from the action of velocity pressure, including mathematics of mass transfer to dissolved gas, comes from the water treatment field (Scardina 2004; Scardina & Edwards 2006). Scardina (2004) reports the degassed nitrogen attaches to flocculants, inhibiting the settling process. A water treatment facility provides easier observation and modeling of velocity induced bubble formation; but a filter bed made of sand is an analogous process to a natural spring discharging through porous media at the spring outlet. Scardina (2004) and Scardina and Edwards (2006), discuss how water accelerating through filter media (sand) causes air binding, where the degassed nitrogen adheres to the filter media, blocking the pores. The same bubble obstruction phenomenon occurs near wells in aquifers (Davis & DeWeist 1966). Additionally, the gas bubbles in aquifers have been

found to form an aquitard, mirroring the results of the work on sand filters in water treatment systems (Ryan et al. 2000; Amos & Mayer 2006).

A suitable mathematical approximation of the local pressures in a turbulent flow regime may be obtained using a multiphase version of Darcy's equation, the Navier-Stokes equation, mass balance, and the SIMPLE algorithm (Semi-Implicit Method for Pressure). This system of equations requires numeric methods to solve with the application of fluid dynamics modeling such as TOUGH2 EOS3 (Pruess et al.1999). This numeric model suitably calculates two-phase conditions of air dissolved in water. By creating a model aquifer in TOUGH2 that includes a high permeability outlet (simulating a karst tube or fracture), the pressure of the groundwater can be seen to decrease in the conduit and, correspondingly, the dissolved air changes to free phase.

Numerous springs around the world exhibit a discharge of nitrogen bubbles. Krešić (2007) provides an illustration of pressure-drop bubbles in Honey Creek, Ann Arbor, MI (282). Various springs in the Arbuckle-Simpson aquifer, including Byrds Mill Spring and Nelson Spring near Ada, OK, produce nitrogen bubbles (Christenson et al. 2009) that may be of this type. Many springs with nitrogen bubbles occur in karst formations, but it is not a prerequisite. Notably, mound springs, including one known as The Bubbler in South Australia, exhibit regular bubble discharge from the Bulldog Shale (Thompson & Withers 2002).

Type IV – Soda

The conceptual model for the presence of Soda (IV) bubbles begins with groundwater in the presence of heat and / or pressure. The heat and pressure drive the

chemo-physical process of gas super saturation as well as the facilitation of chemical reactions with minerals e.g. marine carbonate dissolution to CO_2 (Lewicki et al. 2013). The heat and pressure allow for dissolution of the CO_2 into the water in quantities above the saturation concentration at atmospheric pressure. The result is bubbles in the form of semi-persistent effervescence when these supersaturated waters reach the surface at a spring discharge.

Mineral springs contain dissolved mineral matter in sufficient quantity to impart definite taste (American Geosciences Institute 2016). Soda springs are a sub-set of mineral springs, but are not well defined in the literature and absent in the American Geosciences Institute Glossary. Soda Springs take their name from dissolved sodium bicarbonate; when super saturated, the waters effervesce carbon dioxide gas (Crook 1899). Effervescing water will continue to bubble (for a time) when removed from the spring, unlike Bernoulli (III) bubbles. Henry (1803) provided the first major treatise on the physical phenomenon of the solubility of gases in water and is the namesake of Henry's Law. While all free phase gas discharges require super-saturation, the effervescence of a soda spring is a defining characteristic of this discharge.

Anderson provides one of the earliest accounts of bubbling mineral springs, including chemical analysis, in his work in California (1890). Anderson describes the Bartlett spring as "…continually bubbling up with great force, resembling a *boiling* spring." (Anderson 1890) However, in 1888 the temperature was found to be 54° F [12.2 °C] therefore the water was not in fact Boiling (VI) but rather the CO_2 was ebullating. The phenomenon of effervescence, characterized by the presence of a supersaturated gas, provides the context for Soda (IV) bubbles in this categorization system.

Perhaps the most famous example of Soda (IV) bubbles comes from the Perrier mineral water source spring near Vergèze, France. The Perrier spring produces over 100,000 liters per hour of carbonated water. Water from the Vergèze spring contains 3.5 liters of CO_2 per liter of water (Fox 1988); therefore the CO_2 in Perrier is under ~3.6 bar (360 kPa) of pressure and meets the EU definition of sparkling. The head definitions for soda water and sparkling wines provide the only literature regarding the hydraulic head of free phase gasses. The namesake of soda springs is Soda Springs in Idaho, which exhibits CO_2 flux from the spring water up to 1,147 g m^{-2} d^{-1} (Lewicki et al. 2013).

Deep Bubble Facies

Free phase gas facies of Types V-VII, as shown in Figure 2, tend to occur in relatively deeper formations The gas discharges of facies Bituminous (V), Water Vapor (VI), and Mantle Gas (VII) are associated with depth, where connection with geothermal heat sources or gas from the mantle is essential for formation. For the purposes of this categorization system, deep refers to the source formation commonly being below the base of treatable fresh water.

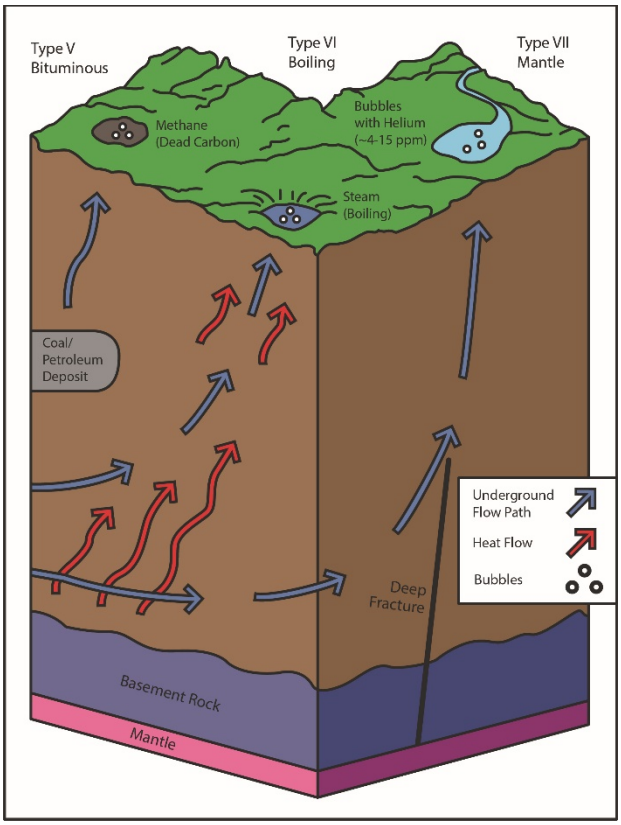

Figure 2. Bubble Facies V-VII.

Type V – Bituminous

The conceptual model for Bituminous (V) free phase gas discharge is the aquifer having contact with deposits of bituminous materials (coal, free oil, oil shales, etc.) producing methane or natural gas bubbles originating from the thermal desorption of bitumen (Schoell 1988). Bituminous (V) bubbles are methane with a dead carbon composition (δ13C -25.4% to -76% with ethane) (Schoell 1980). Marcus *Vitruvius* Pollio described springs of bitumen "…these, though cold, seem, nevertheless, to boil" (Pollio/Rowland c. 15 B.C.E/1999) and provided Darcy with seminal knowledge of springs (Darcy/Bobeck 1856/2004). The Bituminous (V) discharges are characterized by

their fire hazard near the spring orifice, “Methane coming out of solution may accumulate and present a fire or explosion hazard.” (Davis & DeWiest 1966 p. 115). This is also a hazard for Biogenic (I) discharges. The methane volume produced as Bituminous (V) discharges is typically much greater than the volume produced by Biogenic (I) ones.

Early research in Japan describes that methane above its saturation concentration can create bubbles and may strip dissolved nitrogen and argon as they migrate into the methane bubbles, thereby altering dissolved gas levels and analysis (Sugisaki 1964). Another area of research related to methane is seepage around wells, bubbling in mud or water. This has the possibly of contaminating water supplies (Rich et al. 1995). Bituminous (V) discharges may manifest in other, more unusual forms. Additionally, prehistoric Bituminous (V) bubbles may leave a record as fossil evidence of methane vents containing microscopic fossils of methanogens (Kauffman et al. 1996).

Due to the commercial value of natural gas, seeps and bubbles of methane have been of interest to prospectors as well as scientists. An early account in America states, “At Rome [PA], eight miles north-east of Towanda, is a fine mineral spring, impregnated with sulphur, iron, &c. Inflammable [i.e. highly flammable] gas arises in large bubbles from the bottom.” (Geological Society of Pennsylvania 1832 p. 201). This observation occurred 27 years before the first U.S. oil well (the Drake Well) was installed in nearby Titusville, PA.

Contemporary research regarding Bituminous (V) bubbles occurs in Greece with investigations into methane seepage in the northwest Peloponnesus petroliferous basin centering on the Kaiafas Lake Spring, Greece (Etiope et al. 2006), and in the Appalachian basin where methane flux in springs has been investigated (Etiope et al. 2013). Another

well-known example of Bituminous (V) discharge is the La Brea tar pits in southern California and their methane seepage (Farrell et al. 2013). Similar shallow examples of the Bituminous (V) category exist, but the facies is evaluated based on the common origin of deep bituminous deposits.

Type VI – Boiling

The conceptual model for the presence of the Boiling (VI) facies begin with sub-surface waters contacting rock heated by the asthenosphere to a temperature above the boiling temperature of water at atmospheric pressure. Thermal springs, or hot springs, of sufficient temperature provide Boiling (IV) gas discharges. Jean-André De Luc (1772) provided the first major treatise on the physical phenomenon of thermal bubbles. He described the bubbles from dissolved gas as, "*petite bulle*" (De Luc 1772 p. 48), appearing prior to a full boil and producing bubbles of the formerly dissolved gasses. However, the defining characteristic of the Boiling (VI) facies is phase change of the solvent (i.e. water), not the solute (i.e. nitrogen). Given the pressures at depth, the water may stay in liquid phase and be superheated until it travels to a lower pressure region at or near the surface where bubbles form.

Difficulty in establishing early descriptions of this type of bubble originates from the variability of terminology in the existing literature. True scientific exploration into the phenomenon of *Magmatic Waters* began in the early 20th Century, as summarized by Tanton (1915). Thomas Short described Bingham Well in England as producing "large balls or bubbles of heated air" (1734 p. 44). This is not truly a boiling spring since the hottest spring in England is Bath at 96 °C at depth (Gallois 2006). Moorman (1867) gives

several accounts of thermal springs, referencing the earlier work of Dr. LeConte's *Account of some volcanic springs in the desert of the Colorado in southern California* (1855). LeConte describes "boiling mud" that "ejects steam." Moorman provides commentary on similar formations in Iceland and Crimea, suggesting earlier work on the subject. The most prominent example of boiling springs in America is the Heart Lake Geyser Basin (HLGB) in Yellowstone National Park. While Cook (1870) provided the first scientific description of Yellowstone and its waters, Lowenstern et al. (2012) report superheated water at 205 °C in their description of the thermal waters of the HLGB.

Type VII – Mantle Gas

The conceptual model for the Mantle Gas (VII) facies begins with a connective path for gasses from the mantle (e.g. helium) to the shallow groundwater and eventually emerging at the surface. While Boiling (VI) bubbles may occur in conjunction with mantle gas, mantle gas bubbles are distinct from thermal bubbles in composition and origin. Boiling (VI) requires geothermal heat whereas the Mantle Gas (VII) facies originates from depth and may transport sufficient distance to appear without excess heat. While helium is not the only, nor the dominant gas from the mantle, it is the characteristic gas for this facies.

Emanuel Mazor and Gerald Wasserburg (1965) provided the first major study to indicate the phenomenon of mantle gas discharge. In their study on gas discharge from Yellowstone and Lassen, Mazor and Wasserburg (1965) expand on the work of Craig et al. (1956), providing a methodology for sample collection and analysis of bubbles. Mazor and Wasserburg's study includes the analysis of a cold ebulating lake, yielding 14.4 ppm

of helium of non-atmospheric origin. Craig et al. (1978) continued research on the helium connection to the mantle in springs in Lassen and Yellowstone, showing a clear mantle connection using Helium isotope ratios ($^3He/ He$).

Sugisaki and Sugiura (1986) demonstrated a connection in the increased rate of bubble generation of endogenic gases prior to a major earthquake in Japan in 1984. Sugisaki and Sugiura show a relationship between pore pressure in the crust and changes in the gas generation rate and set forth the concept of an earthquake early warning system using gas chromatography to measure changes in He/Ar and CH_4/Ar ratios. A more recent study by Bräuer et al. (2011) in the western Eger Rift in the Czech Republic continues with the pore pressure theory and links degassing of endogenic helium with earthquake swarms.

Bräuer et al. (2013) also describe one of the most important examples of springs emanating mantle gas bubbles that are in the Eifel area of Germany, where 25 degassing locations are present. The researchers were able to show the presence of two distinct isotopic signatures from depth; the waters were between 2 °C and 21 °C. The gas analysis coupled with the relatively low temperature of these springs indicates a mantle connection without the necessity for magmatic proximity. Crossey et al. (2009) found free gas phase, as well as dissolved inorganic carbon, indicating an endogenic source for CO_2 and helium in the Colorado Plateau-Arizona Transition Zone. The research provides methodology for determining the contribution of epigenic (meteoric) and endogenic (deep) gas in the combined spring discharge. Ricketts et al. (2014) discussed mantle-derived helium in travertine discharges in the Albuquerque basin, indicating up to 25% of the helium came from a deep source.

Bubbles with Complex Facies

The categorization system defines seven mechanisms for the evolution of bubbles in springs and examples of springs that follow these behaviors. However, bubbling springs may exhibit more than one distinct facies. This section provides examples of mixed facies springs and clarification on the methodology for formally describing the facies present.

CO_2 may act as Bernoulli (III) bubbles when concentrations are near or slightly above saturation, as is the case with some mound springs in South Australia (Keppel et al. 2011). In the South Australia study, the team concluded deep pools of spring water at the surface reduced discharge turbulence and might inhibit CO_2 degassing. A potential variable is the generation of bubbles through a change in head creating non-Darcian flow versus a velocity pressure-drop (Nowamooz et al. 2009). High fluid velocity in a porous medium will likely characterize Non-Darcian multiphase flow, i.e. Bernoulli (III) (Zeng & Grigg 2006).

Soda (IV) and Boiling (VI) facies may appear together in hot springs. These mixed bubble facies may appear as geysers or mofettes. A mofette is a small opening where CO_2 is emitted in an area of late-stage volcanic activity (American Geosciences Institute 2016). Mofettes and geysers are special cases of bubbling springs where heat and pressure drive the exsolution process.

When investigating springs, the presence of Boiling (VI) bubbles provides clear evidence of heated (likely superheated) water and therefore the presence of a geothermal zone. A magmatic reservoir may be present in these superheated conditions with the possibility of Mantle (VII) discharge. The gas phase will achieve equilibrium with the

constituents in the magma and can provide a means of identification of the volatile components of the magma through sampling the free gas phase (Ellis 1957; Giggenbach 1980).

One of the most famous of thermal springs, Bath, Somerset, England (Cunliffe 1984) is not a boiling spring as the maximum temperature at depth is 64-96 °C (discharge 45-46 °C) (Gallois 2006). The presence of hydrogen sulfide (H_2S) gas bubbles (Edmunds 2004) makes Bath an ebulating spring rather than a boiling spring and therefore classified as Bituminous (V) bubbles. A true boiling spring in this classification system will degas other dissolved gas species, providing for more than steam in the bubbles (De Luc 1772). This is the case with carbon dioxide and hydrogen sulfide degassing in Brimstone Basin, Yellowstone National Park, Wyoming (Bergfeld et al. 2012). The degassing effect is not limited to Bernoulli (III) bubbles.

Travertine formation at hot springs, including bubble travertine from degassing of carbon dioxide, is another factor illustrating the complexity of classifying free phase gas facies in some springs (Guo and Riding 2002). Bubble travertine is, "[g]as bubbles coated by rapidly precipitated calcium carbonate" (Guo and Riding 2002, 168). However, the gas discharge occurring during the formation of bubble travertine arising from mineral dissolution is categorized here as the Soda (IV) facies.

The work of Lewicki, et al. (2013) indicates soda springs may be comprised of Mantle (VII) discharge in addition to Soda (IV) discharge. Crossey, et al. (2009) confirms endogenic (deep) and epigenic (surface/meteoric) CO_2 are commonly found together as dissolved inorganic carbon. While both Soda (IV) and Mantle (VII) facies may result in supersaturated concentrations of dissolved gas, the origin of the bubble is used for this

categorization system. Dissolution of minerals by water characterizes the Soda (IV) facies rather than the deep connectivity producing Mantle (VII) discharges. The commonality of multiple bubble facies occurring in conjunction adds to the difficulty in determining free-gas origin.

The soda springs in Soda Springs, Idaho are examples of both a well-known Soda (IV) spring, as well as a significantly studied spring. Lewicki et al. (2013) provided several measurement techniques and reported three sources of dissolved CO_2 in the spring, Biogenic (I) gas (3%), carbonate mineral dissolution (35%) Soda (IV) gas, and deep sourced (62%) Mantle Gas (VII) discharge. Lewicki et al. (2013) also demonstrated investigating free phase gas facies requires significant attention to detail as multiple facies could occur simultaneously, providing insight into the complex flow lines of the aquifer or converging aquifers.

Another complex phenomenon is seismically triggered microbial methane (Bräuer et al. 2005). Unlike the more typical biogenic methane, which is derived from decaying organic matter, Bräuer et al. (2005), showed excess hydrogen from the seismic activity triggers increased microbial activity. The excess hydrogen forms Mantle Gas (VII) bubbles, and the microbial methane forms Biogenic (I) bubbles at depth, producing both facies at the spring discharge.

Mariner et al. (2003) stated excess nitrogen has a possible non-atmospheric origin. Typical nitrogen/argon (N_2/Ar) ratio values for atmospherically derived nitrogen in the range of 40-80, where N_2/Ar values for volcanic sources are orders of magnitude higher. Microbial denitrification can be a significant source of dissolved nitrogen in

surface water sediments (Böhlke et al. 2009). While nitrogen bubbles are typically Bernoulli (III) facies, they may be Biogenic (I) facies if caused by denitrification.

Future Work

This proposed classification scheme is an attempt to improve two aspects of free phase gas research in groundwater. First, being more precise with free phase definitions and usage allows researchers to compare across datasets with a language that is more uniform. Second, the scheme provides a similar language to treat the types of free phase gas phenomenon that researchers are evaluating in comparison to other locations worldwide.

As with any classification scheme, future work will cause a reevaluation of the named free gas facies or the addition of others. For example, the authors left out a potential category of glacial bubbles formed by gas introduced during glacial melt processes (Anderson, 2004). This was due to a limited amount of existing research at the time this review was performed. Additionally, the proposed classification covered the minor gases that might emanate with others that could be classified in the existing scheme. Future work may demonstrate that the presence of a particular gas composition is indicative of a unique groundwater process and need a separate bubble facies.

Summary

Early research gave significant attention to bubbling springs using simple observations and a curiosity for novel waters. Contemporary researchers have started to apply advanced instrumentation to the analysis of collected gas samples. We have offered seven phenomena that answer the question, “Why springs bubble?” and provided for a

facies categorization system for free phase gas discharge from groundwater based on a review of the literature. The facies convention and clarification of terms provides a framework to establish a vernacular and facilitate the exploration of this phenomenon in springs, in the hope of fostering defined lines of investigation to facilitate the exchange of knowledge and advancement of the field. By exploring the free phase gas discharges in springs, in addition to the dissolved phase, researchers will gain additional insight into the inner workings of aquifers and reduce errors associated with dissolved phase gas sampling.

CHAPTER III

METHODOLOGY

An Instrument for the Determination of A Hydropneumograph in A Bubbling Spring

Article Publication: Accepted by Groundwater (Agnew et al., 2019), used here in accordance with the Wiley Publishing Services Copyright Transfer Agreement – Permitted Uses By Contributor.

Authors: Robert J. Agnew, Todd Halihan, Lantz Holtzhower, and Brian Norton

Numerous springs have been reported to ebullate gas (free phase gas discharge) (Woodward 1910; Thompson & Withers 2002; Krešić 2007; Agnew & Halihan 2018). Described in this methods note is a field deployable device that is capable of economically measuring the gas phase discharge at a bubbling spring. This type of device is important for groundwater studies to provide data on gas mass flow rate and composition. The ebullition occurring at a spring discharge may act to strip out dissolved gases, which would introduce error into a dissolved gas analysis (White et al. 1963; Baird

et al. 1979; Patoczka & Wilson 1984; Lucchetti & Gray 1988; Vroblesky and Lorah 1991; Mariner et al. 2003). Failing to account for the free gas phase may introduce significant errors in determining the total gas present and thereby alter measurements of interest, such as water age dating (Taran 2005).

Understanding spring discharge of water over time has provided significant insight into groundwater flow, but similar measurements of the gas discharge are generally unavailable as temporal data. The proposed apparatus provides a method to both capture gas for constituent analysis and to measure the mass flow rate. Combining gas mass flow rate with gas constituent analysis allows for proper mass balance in the computation of gas ratios.

In order to deploy an instrument into the field, it must be reasonably portable and capable of measuring the flow rate of both the gas and liquid phases. The apparatus must also record environmental data, including temperature and pressure, to provide adequate information to detect changes in gas generation rate not attributed to changes in water flow or atmospheric conditions. The apparatus must be size scalable to capture gas and water mass discharges from various magnitude springs. Finally, it would be useful if the apparatus is relatively affordable if it is to be used in the field for an extended duration to capture seasonal flow variation.

For the sake of portability, an instrument that is capable of directly measuring bubbly mixed-phase flow would be preferred. Direct bubble measurement is difficult (Taran 2005) and requires significant assumptions for mathematical modeling (Brennen 2005; Lavenson et al., 2016; Daniel 2018). Measuring water flow that contains entrained gas introduces error into conventional measuring devices, such as paddlewheel, pressure

drop, turbine style, etc. (Hanson & Schwankl 1998); however, water velocity in bubbly mixed-phase flow has been successfully measured using an electromagnetic flow meter (Leeungculsatien & Lucas 2013). Unfortunately, the electromagnetic flow meter designed for bubbly mixed-phase flow is a sensitive piece of equipment that is presently only suitable for laboratory measurements.

Successful bubble-scale measurements of gas in the mixed phase have been accomplished in the nuclear industry via ultrasonic void measurement (Aritomi et al. 2000; Filho et al. 2009). High performance measurement of gas volume in bubbly mixed-phase flow for natural gas extraction has been accomplished using a four-sensor conductivity probe (Pradhan 2010). These bubbly mixed-phase flow instruments are designed for use in high-temperature and high-pressure environments making them a relatively expensive sensor technology that is more applicable to the non-Darcian conditions of natural gas extraction wells (Zeng & Grigg 2006). An intriguing developmental method of using acoustics to measure bubble generation is reported by Czerski and Deane (2010). Other techniques, including a fiber optic probe (Lim et al. 2008) are available. Ultimately, all these methods are costly.

In light of the deficits related to direct measurement of bubbly mixed-phase flow, and for the purposes of practicality and economy, a simple device that separates the flows of gas and liquid and provides for easy measurement of each separate phase is required. Koch et al. (2003) provides an excellent diagram of a phase separation device permanently installed on a spring in the Upper Vogtland (Germany) that allows for real-time collection of the flow of both phases. This permanent installation required pouring of concrete and other expensive infrastructure that is not feasible or may not be allowed

at a field site. The basic concept of separating the two phases of flow for measurement is reasonably achievable in field conditions.

The design of a phase separating gas mass discharge logger requires several design considerations. First, an estimate of the gas and water mass flow and flow velocity is needed in order to size and calibrate the flow measuring devices. Estimates of gas flow rates tend to be biased towards the free phase gas bubbles that are visibly present and do not accurately include gas flux across the bulk interfacial area of the spring discharge. If the supersaturation ratio is known, the flux may be estimated (Wanninkhof et al 2009). Failure to properly estimate the total gas flux, and the corresponding sampling tube and pressure relief vent could increase the pressure in the device and diminish responsiveness to changing gas flow rate, or cause the structure to float and lose containment of the gas phase discharge.

A crude field estimate of gas discharge using a funnel device has been successfully used to collect the gas phase from a spring for laboratory analysis (Sugisaki & Sugiura 1986; Fox 1988; Mariner et al. 2003; Bräuer et al. 2005; Bräuer et al. 2011). In an accurate low flow instrument, the humid gas flow will need to be dried prior to measurement. Additionally, the gas mass flow rate may be influenced by differential temperaures and pressures between a collection structure (shroud) and the atmosphere, known as the stack effect (Atkins & Escudier 2013). Stack effect has been shown to affect radon flux (Saiway et al. 2006), transport of vapors and aerosols in buildings (Madrzykowski & Kerber 2009), and chemical vapor intrusion into buildings from contaminated groundwater (Song et al. 2014). Mitigating the stack effect within the phase

separator can be accomplished by covering/insulating the apparatus to prevent solar load and minimizing the size of the collection funnel.

Finally, bubbles in springs do not appear in a steady rhythm, but rather at an irregular pace. Many karst springs are known to have episodic or rhythmic water flow or siphon effects (Bonacci & Bojanić 1991). These variable springs may have regular or non-linear oscillations in flow, and it follows that bubbles generated in karst springs may possess a similar variability. Bonacci & Bojanić (1991) summarize the work of many researchers and demonstrate the conceptual model of chambers and syphons to create episodic flow patterns. A spring upwelling into a gravel bed may have episodic ebullition due to gas accumulating in the interstitial space between aggregates until sufficient buoyancy is achieved and a cascade of bubbles emerges. Due to the episodic bubble generation rate, a direct correlation between liquid flow and gas flow is infeasible; therefore, measurement data for the gas and liquid flow requires some temporal averaging.

A prototype phase-separating gas and water flow-measuring device was constructed and deployed at the Little Bubbler Spring located within the Nelson Spring Complex. The Nelson Spring Complex is located on the Arbuckle-Simpson Ranch near Connerville, OK. The Little Bubbler Spring is a fifth magnitude spring during peak flow and a sixth magnitude spring during base flow. The spring is located at 34°27'26.23"N, 96°40'6.36"W. The spring was selected due to its slightly elevated position related to a nearby steam, moderate water flow rate, heavy shade, and its intermittent yet steady stream of bubbles. The spring discharges from the fractured and karstic Arbuckle-Simpson aquifer. The isothermal nature of this spring (16.4 +/- 0.2 ˚C) provides an

excellent field site as gas volume dependencies on spring temperature variations are nearly eliminated.

Methodology

The mass measuring devices consist of a weir for determining the mass discharge of water and a phase separator for determining the mass discharge of gas. These instruments were installed at the spring orifice. The methods are presented for determining the mass flow rate of water followed by the approach to measure the mass flow rate of gas. The power supply and data logging apparatus are also described. Next, the field deployment of the apparatus is described. Finally, additional features were added for sampling gas composition.

Water Mass Flow Rate

Water discharge from the spring is measured using a thin-plate V-notch weir (ASTM D5242-2013) (Figure 3). The weir has a V-notch θ of 28.09 degrees, 12 inch high, made from 16 ga. (0.063 in, 0.16 cm) steel plate. The hydraulic head and water temperature were measured using a Solinst® 3001 Levelogger LT F15/M5 ± 0.3 cm (0.05% FS - ± 0.05 kPa) with temperature sensor accuracy of ± 0.05 °C and resolution of 0.003 °C. Data were recorded every five minutes for the planned 28-day test period.

The weir head is corrected for local atmospheric pressure using a Solinst® 3001 Barologger F5/M1.5 (0.05% FS - ± 0.05 kPa) with temperature sensor accuracy of ± 0.05 °C and resolution of 0.003 °C. Data were processed using Levelogger software version 4.3.3.

Water mass flow rate from the weir flow was then calculated using the Kindsvater-Shen equation (U.S. Bureau of Reclamation, 2001) shown in Equation (1).

(1)

$$Q = 4.28\, C \tan\left(\frac{\theta}{2}\right)(h + k)^{\frac{5}{2}}$$

Where:
Q = Discharge (cfs)
C = Discharge Coefficient
θ = Notch Angle (degrees)
h = Head (ft)
k = Head Correction Factor (ft)

Figure 3. Apparatus Installation.

Legend: Water flow from the spring migrates upward on the photo from the shroud to the stream channel past the weir. Gas flow is collected in the shroud and is routed to the instrumentation box.

As V-notch weirs are subject to obstruction by floating debris such as leaves, they must be regularly cleaned. As this weir was installed in a remote location, regular hand cleaning as recommended by the ASTM standard was not practical. Therefore, an

automated weir cleaning arm was installed. The arm was constructed of an 11-inch long metal rod attached to the drive of a waterproof solenoid motor (Fan Model FS-20W) with a torque of 16.0 kg-cm (1.16 ft-lbs). The rod swept up and back through the weir notch once per hour as controlled by a WitMotion motor controller driver board (adjustable relay). Power to the board and solenoid motor was Tobsun EA15 DC converter to produce a 5-volt leg on the main 12 V power system.

Gas Mass Flow Rate

The gas mass flow rate instrument included a gas capture shroud, solar power supply, and electronic instrumentation including a thermal mass flow sensor for gas mass measurement. These instruments were installed at the spring discharge. Along with enabling the water mass flow measurement, the weir creates a pool for the placement of the gas shroud (Figure 4). The gas shroud is connected via tubing to the thermal mass flow sensor in a protective field enclosure.

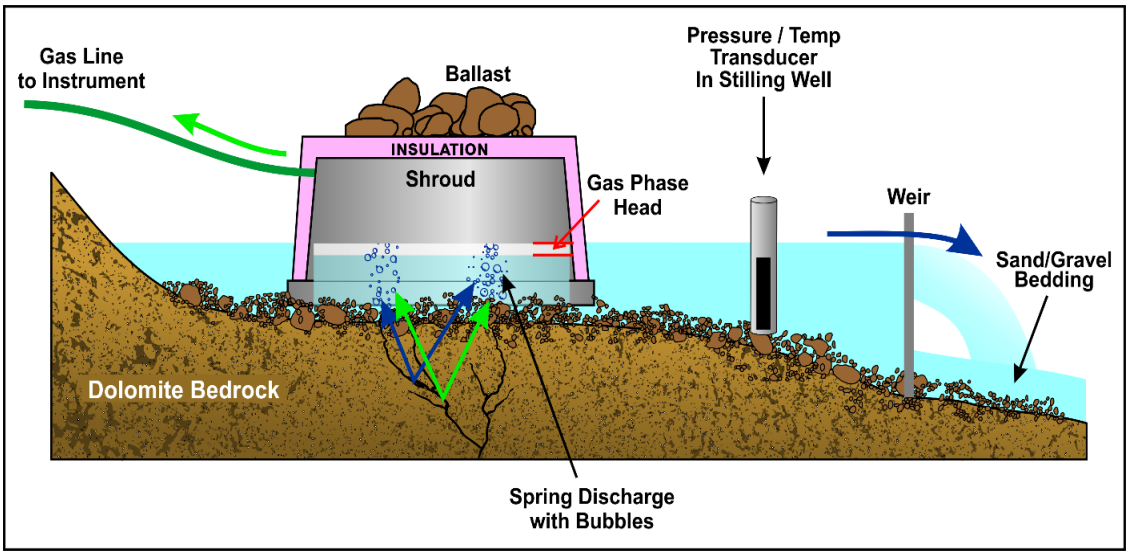

Figure 4. Gas Collection Apparatus Profile View.

Legend: Blue arrows indicate water flow and green arrows indicate gas flow.

The gas ebullition capture shroud is placed over the point of separate phase gas discharge at the spring orafice. The shroud is a round 1.83 meter (6-foot) diameter stock tank, 0.6 m (24 inches) tall, with a ¾ inch NPT drain outlet. The drain of the inverted stock tank, at the high point of the shroud, acts as the connection for the tubing leading to the mass flow sensor. Given the 2.63 m^2 surface area of the top of the shroud, the uplift force on the shroud equals approximately 4,500 N (1,000 lbf) at the cracking pressure; ballast weighing 25% greater than the reactive force was placed upon the shroud. Flow in the system is derived from gas accumulating in the shroud, displacing water into the pool and creating a water level differential (gas phase head) between the shroud and pool (Figure 5).

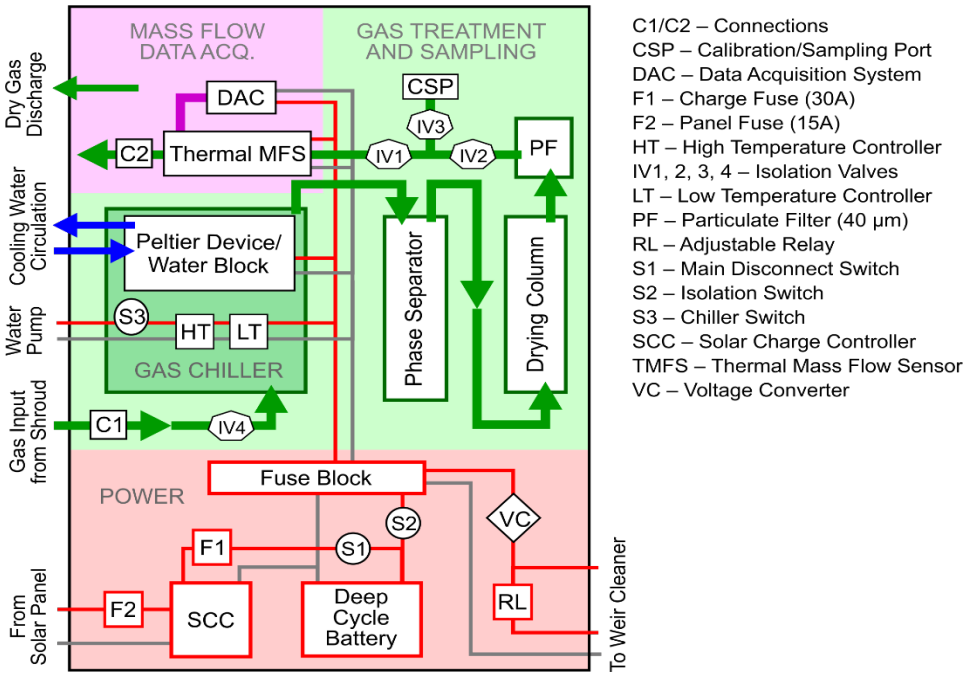

Figure 5. Instrument Box Layout.

Legend: Blue arrows indicate water flow for cooling and green arrows indicate the direction of gas flow through the system.

An Aalborg XFM17 thermal mass flow sensor (TMFS) with totalizer is used to measure the gas discharge collected by the shroud. A TMFS was selected due to its high precision and accuracy at very low flow rates. Other flow measuring technologies are available but lack the ability to measure at low flow (e.g. orifice plates). The TMFS was factory calibrated using dry nitrogen.

The nitrogen concentration in the water of Nelson Spring Complex is reported by Christenson et al. (2009) as 22.03 ccSTP/kgH_2O. Therefore, nitrogen was selected as the reference gas for the TMFS due to nitrogen being the dominant gas in the Nelson Spring Complex. A whole gas sample was analyzed by the USGS Noble Gas Laboratory in accordance with Techniques and Methods 5-A11 (Hunt 2015) confirming 84.2% by

volume N_2 in the discharging gas phase, with 11.8% O_2, 2.6% CO_2, 1% Ar, and the balance of trace gases.

Flow in the system is derived from gas accumulating in the shroud, displacing water into the pool and creating a water level differential between the shroud and pool. The gas is conducted from the shroud via ½-inch o.d. polyethylene tubing 30 feet to the equipment box via a series of bushings and adapters. The tubing is run inside ¾-inch nominal diameter flexible metal conduit to protect the tubing from mechanical damage or animal tampering. At the connection to the shroud a ¼ turn shut-off valve is provided upstream of a pressure relief valve (PRV). The PRV is a 3/8" UCM13-4BP-35-.25 nickel plated brass atmospheric relief valve with a Buna seal, polypropylene poppet, fritted dust cap, and a cracking pressure of 1700 Pa (0.25 psid, 6.9 in H_2O). The cracking pressure was determined by doubling the highest recorded pressure on the line of 750 Pa (3 in. H_2O). The pressure in the system is the result of friction loss in the tubing, conditioning, and measuring train.

In order to prevent thermal effects from sunlight and atmospheric temperature variability, the shroud is insulated on top with ½" metal foil backed foam insulation board (placed below the ballast). The sides of the shroud are wrapped with two layers of 3/16" metallized thermal bubble roll. The foil/metalized insulation barrier reflect radiant heat from solar load which would otherwise affect the gas pressure in the shroud. Temperature in the shroud is also maintained by the constant flow of cold water from the spring water discharge. The gas line coming from the shroud to the instrument box is wrapped in foam pipe insulation. Insulating the line prevents water condensation in the

winter and excess heating in the summer, which can lead to higher humidity in the sample gas.

The instrument box (Figure 5) supports the system power supply, gas conditioning systems, thermals mass flow sensor (TMFS) and Data Acquisition System (DAC). The TMFS has a calibrated range of 0 – 1 standard liters per minute (sLPM) ±1% full scale. The sensor is powered by 11 to 26 volts DC and outputs a 4-20 mA analog signal. The principle of operation of the TMFS is based upon heat transfer. Gas flow is separated into two paths, the main path and the capillary path. Heat is introduced to the capillary path by a precision heater coil and heat transfer is measured downstream by an analogous coil. As gas passes the coils, the heat loss is correlated to the specific heat of the gas resulting in detection of total mass flow (Aalborg 2016).

The TMFS has a 10-point factory calibration and includes a certificate of calibration that is used to correct flow measurements. The TMFS is fitted with over-sized 3/8 inch compression fittings to reduce friction loss in this low-pressure system. The 3/8 inch connectors are coupled to 3/8-inch outside diameter (o.d.) polyethylene tubing. Inside the housing, the 3/8-inch tubing is connected to a series of brass valves (Figure). The TMFS is calibrated with dry nitrogen. Correction for water vapor laden gas less than 70% relative humidity is not needed. Moisture content does not affect the accuracy beyond 1% full scale; however, the capillary tube has a small diameter and is subject to condensation blockage if the water vapor saturation exceeds 70%.

The gas sampling line requires gas conditioning to reduce the humidity of the incoming gas feed. The gas sampling line conditioning included a gas chiller/moisture condenser, phase separator, and a drying column filled with Drierite® desiccant (Figure

5). The gas chiller is a heat exchanger made from four-inch square, 12-inch tall by 4-inch square aluminum tank with ¼-inch thick walls. A coiled ¼-inch copper tube 20-feet in length passes through the chiller box that is filled with water. Water is added through a ¾-inch NPT opening in which is interested a brass plug with a waterproof thermocouple. The chiller box is insulated with two layers of ¾ inch thick Extruded Polystyrene (XPS) foam board.

The heat exchanger is cooled by a Peltier device. The Peltier cooler measures 40 mm x 40 mm x 3.71 mm providing 53.2 Watts of cooling and drawing 4.8A. The Peltier rejects heat to an aluminum water block of the same dimensional area. Water is supplied to the block via 7/16" OD tubing connected to an Aubig DC40-1250 Brushless Magnetic Drive Centrifugal Submersible Water Pump that provides 500 liters of water per hour. The pump is placed in the spring pool and provides 16.5 C water for cooling. Affixed to the pump is a filter box to prevent aquatic fauna (leeches) from clogging the impeller.

The cycled water is returned to the pool as to not affect water level measurement. The water lines are covered in an opaque material to prevent algal growth. In order to conserve power, the Peltier chiller is controlled by a programmable temperature controller W1209 connected to the waterproof thermocouple in the chiller tank. The low temperature controller is set to begin chilling at 4° C and turn off at 2° C. A second high temperature controller is attached to the water cooling block to detect a loss of water and turns off the chiller if the block temperature exceeds 50° C.

Once the gas flow leaves the gas chiller it enters a phase separator. The phase separator is a 16 fl. oz. Nalgene bottle with bulkhead fittings through the threaded lid. The phase separator collects condensed water from the gas chiller and passes the dried

gas to the drying column extending the service life of the desiccant. The clear PVC drying column is 3” in diameter, 22 inches tall, filled with five pounds of 8-mesh indicating desiccant. The desiccant is made from calcium sulfate with cobalt dichloride as the indicator of moisture breakthrough (Drierite®); the sample line is equipped with a 40-micron filter after the drying column to ensure dust from the Drierite® does not clog the capillary tube of the TMFS.

Use of the gas drying column extends the ambient operating temperature of the TMFS from 0 °C to 50 °C (32 °F to 122 °F) without the column, to -10 °C to 50 °C (14 °F to 122 °F) with the drying column. The average low temperature in Ada, OK near the test location, in the coldest month (January) is -2.8 °C (27 °F); which is in tolerance for the TMFS. However, the record low in Ada, OK is -23°C (-10 °F), which required monitoring via the built in temperature sensor on the DAC during the development of the instrument. The waste heat from the solar charge controller assisted in maintaining the ambient temperature inside the equipment box at acceptable levels.

All the gas measuring components are housed in a Pelican™ polypropylene case model 1650-020-110. The TMFS has an environmental rating per the International Electrochemical Commission (IEC) standard 60664-1 (2007) for Installation Level II; Pollution Degree II. This device cannot be installed outdoors due to moisture sensitivity. The case is designed per IEC 60529 (2013) with an Ingress Protection rating of 67 (IP67), which is dust tight and water tight to one-meter depth meeting the IEC standard.

Penetrations in the case to allow for the sampling line and the electrical lines were sealed with silicone caulking. Since the gas outlet discharges into the enclosure before exiting through a small orifice in the case, the enclosure was effectively purged

with dry nitrogen preventing condensation from the chiller element. This maintained the enclosure at positive pressure with respect to the atmosphere and kept out environmental moisture.

Data Logging and Power Supply

The 4-20 mA data output from the TMFS was recorded by a Campbell Scientific® CR300 data logger with PC200W software (version 4.4.2). The non-isolated 4-to-20 mA current-loop was measured using a 24-bit analogue to digital (A-to-D) converter with an accuracy of ± 0.26% of the reading at a temperature range of -40 to 70 °C. Data from the TMFS were recorded every 10 seconds.

Power was provided to the electronic components of the system by two Renogy RNC-100D monocrystalline solar panels with a maximum power of 100 watts each under Standard Test Conditions with an optimum output of 18.9 V and 5.29 A. Overall panel dimensions of each solar cell are 119.5 x 54.1 x 3.5 cm (47 x 21.3 x 1.4 in). The solar panels were connected to a Renogy Wander CTRL-WND30 charge controller that was connected to two NAPA 8301 deep cycle 12V flooded cell batteries (~105 amp-hour each). The panel and charger were connected by 8 AWG wire routed inside ¾-inch nominal diameter flexible metal conduit to protect the tubing from mechanical damage or animal tampering. The solar power system was designed to provide sufficient power on the shortest day of the year to supply the equipment with the required daily energy consumption. Additionally, the batteries were sized to provide four days of backup power in the event of a power system component failure.

Instrument Deployment and Testing

Once the major components of the system were installed at the field site, the instrument was leak checked and field calibrated. All gas connections were made of brass compression fittings. Several pieces of hardware were integrated into the gas tubing system to allow testing and calibration. This hardware includes system gas connections (C) and gas isolation valves (IV) (Figure 5). The connectors and valves may be configured in several ways to allow for different operating modes and functionality (Table 3).

Table 3. Sampling Train Hardware Configurations

Operation	**Hardware**					
	Connection 1	Connection 2	Calibration/ Sampling Port	In-line Valve 1	In-line Valve 2	In-line Valve 3
Leak Check	Calibration Gas Cylinder	Closed/ Capped	Closed/Capped	Open	Open	Open
Zero/Reset Totalizer	N/A	Closed/ Capped	N/A	N/A	Closed/ Capped	N/A
Calibration	Calibration Gas Cylinder	Open	N/A	Open	Open	Closed/ Capped
Flow Measurement	Shroud	Open	N/A	Open	Open	Closed/ Capped
Whole Gas Sampling	Shroud	N/A	Whole Gas Sampling Vessel (Canister or bag)	Open	Closed/ Capped	Open

The fittings were leak tested by connecting a nitrogen calibration cylinder to the shroud end of the system, opening isolation valves one and three, closing isolation valve two, and capping the discharge line. With the cylinder valve open and the system pressurized, all the gas connections were leak tested using Snoop® liquid leak detector.

The system was field calibrated by zeroing the TMFS then flowing nitrogen from the compressed nitrogen cylinder at three known flowrates. Flow from the gas cylinder was controlled by Premier Industries 2700 series fixed flow regulators with flow rates of 0.3, 0.5, and 1.0 sLPM. The principle of operation of the regulators was a needle valve restricted orifice with a +/- 10% accuracy over the pressure range of the bottle. The regulator was attached via a Compressed Gas Association (CGA) standard C-10 connector to a 1,000 psig cylinder containing 103 standard liters of 99.999% nitrogen. The calibration cylinder was connected to the far (shroud) end of the polyethylene line to account for friction loss in the system. A 3-point field calibration was performed prior to beginning data collection, and again after data collection to account for drift, with less than 5% drift being acceptable (MSHA 2014).

The power supply for the system was tested each time the investigator visited the site. Voltage at the battery was checked as well as voltage coming into the solar charge controller using a standard DC volt meter. The batteries were checked for available current using an ammeter.

Additional Features

The primary purpose for this instrument was the measurement of the mass flow rate of the gas and liquid phases of bubbly mixed-phased flow. While these measurements provide useful data, the full potential of the instrument was met when the data were combined with compositional analysis of the free phase and dissolved phase gasses.

By utilizing connection three (Figure 5) to attach a whole gas sampling device such as an evacuated canister or non-reacting bag, the ebullating gas may be collected for

analysis. A copper tube and clamp sampler may also be used, but has the potential to react with oxygen and other active species. The totalizer on the TMFS was used to determine when it was appropriate to collect a whole gas sample. The shroud must first be allowed to exhaust the background air from when it was installed. Using dilution ventilation equations, purge volumes or time to dilution, values may be calculated (Equation 2; National Safety Council 2012). After calculating the effective ventilation rate of the shroud, the purge time was obtained based upon the flow rate measured by the TMFS. The effective mass flow rate accounts for non-ideal mixing in the shroud, increasing the number of purge volumes necessary to reduce the initial concentration of air.

$$Q' = \frac{Q}{K} \tag{2}$$

Where:

Q' = The effective ventilation rate, liters per minute (lpm)

Q = Actual ventilation rate, lpm

K = A dimensionless mixing factor from 1 to 10 to account for imperfect mixing within the enclosed space, where 1 is ideal and 10 is poor.

Using the effective flow rate, the concentration of the initial air in the shroud at a given time was determined by Equation (3).

(3)

$$C_t = C_i \left[e^{\left(\frac{-Q't}{V_e}\right)} \right]$$

Where:

C_t = Concentration at given time, percent

C_i = Initial concentration, percent

Q' = The effective ventilation rate, lpm

t = Purging time, minutes

V_e = Volume of the enclosure, liters

Solving Equation 2 for time yields:

(4)

$$t = \frac{\left[V_e * ln\left(\frac{C_i}{C_t}\right) \right]}{Q'}$$

By assuming a reasonable K value and using a known shroud volume and flow rate, the purge volumes necessary to achieve the target residual concentration of less than one percent of original air was determined by

(5)

$$V_{p=} \frac{t*Q'}{V_e}$$

Where:

V_p = Purge Volumes

Therefore, 15 purge volumes of the shroud will result in a C_t of 0.7% given a K of 3, or 10 purge volumes with a K of 2. For the device on the test spring flowing nominally

at 0.7 sLPM, once the totalizer reaches 24,500 liters in about 24 days, free gas composition assessment can be assured.

Whole gas samples may be collected by either a vacuum canister or a film bag. Since helium is of primary significance in groundwater analysis, film bags were not appropriate for this application. For example, Tedlar™ bags have a gas permeation rate for helium of 150 cc / (100 in^2)(24 hr)(atm)(mil) compared to the nitrogen permeation rate of 0.25 cc / (100in^2)(24 hr)(atm)(mil) (DuPont 2014). Additionally, film bags have a maximum hold time of before analysis of 48 hours whereas vacuum canisters were stable for 30 days (Eurofins Air Toxics, Inc. 2014), making canisters more practical for remote field collection.

Stainless steel vacuum canisters that have undergone electro-polishing and chemical passivation using the Summa process (i.e. Summa Canisters) are available in one liter and six liter volumes (Eurofins Air Toxics, Inc. 2014). Summa Canisters were fitted with critical orifice style regulators, which allowed for low flow rates (3.8-167 mL/min) that will not induce a vacuum in the shroud and could alter the mass fractions of ebullated gas. A preferred sampling method would use a one-liter Summa Canister with the regulator set to 167 mL/min and a sampling time of five minutes to achieve the target 800 mL sample volume. The collection point, C3 (Figure 5), should be placed after the drying column and particulate filter to eliminate water vapor from condensing in the canister and to prevent particulate blockage of the critical orifice. Alternatively, copper tube sampling using a crimp style cold welder may be used to collect gas samples. However, the copper metal is reactive with oxygen and will alter these measurements along with measurements for reactive species at contamination sites.

The whole gas sample may be analyzed by Gas Chromatography Mass Spectroscopy in accordance with the USGS Techniques and Methods 5-A11 (Hunt 2015). In addition, dissolved gas sampling should occur at the same time of whole gas sampling. Dissolved gas sampling is performed using the copper tube method (Hunt 2015). By using the same analytical technique as used for the dissolved phase gases, the total mass of the dissolved gasses may be calculated. Alternatively, dissolved gas measurement may be achieved by a permeable gas membrane technique (Manning et al 2003; Matsumoto et al. 2013).

Preliminary Results

The flow-measuring device deployed at the Little Bubbler Spring successfully measured gas generation rate and water flow simultaneously. A sample of four days' worth of data is presented as a hydropneumograph (Figure 6) by binning the 10-second data to 15-minute data. For the sample period, the water flow rate was relatively stable with an average mass flow of 0.09 kg/s (1.44 gpm) and includes a handful of higher flow periods with a maximum mass flow of 0.16 kg/s (2.55 gpm). The gas flow rate (mostly nitrogen) oscillated between high and low flow, but without an obvious periodicity. The average nitrogen mass flow rate was 13.19 mg/s (0.63 SLPM or 0.022 SCFM) and ranged from a low of 12.34 mg/s (0.59 SLPM or 0.021 SCFM) to a high of 14.41 mg/s (0.69 SLPM or 0.024 SCFM).

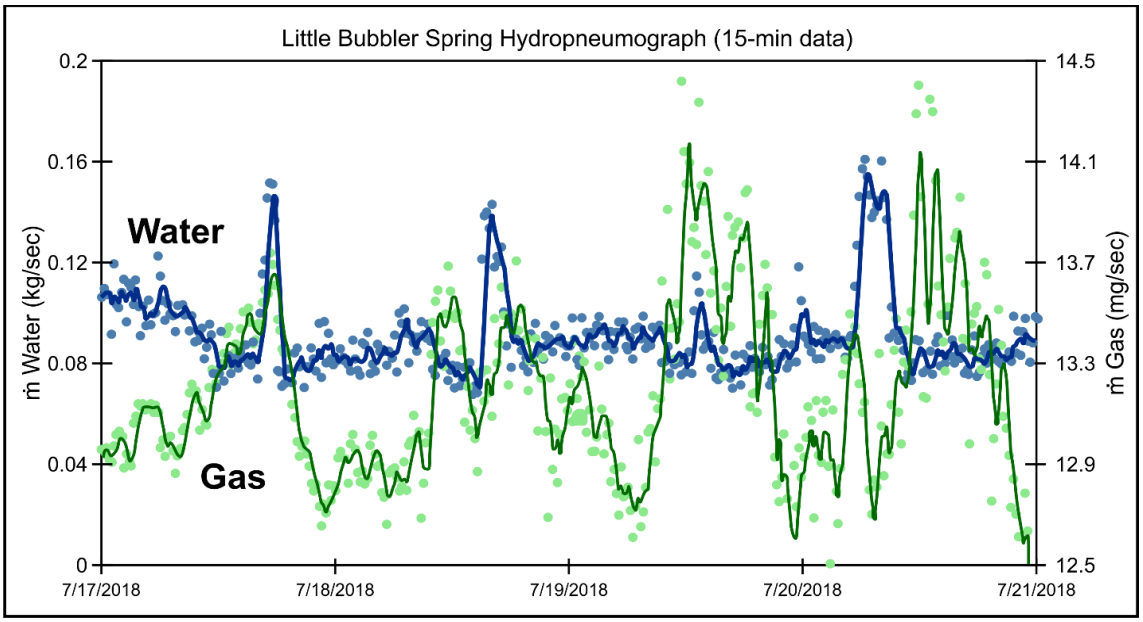

Figure 6. Little Bubbler Spring Hydropneumograph.

Legend: Solid line is a 5-point running average of the individual data points.

Discussion and Summary

The instrument described in this work successfully measured bubbly mixed-phase flow of groundwater from springs and produced a dataset in the form of a hydropneumograph. The instrument was broken up into manageable sized components that may be deployed in the field and provide continuous data collection. By the use of a phase separator, the gas generation rate and the water flow rate were independently measured. These data are necessary for understanding gas mass flow rate or WGR, which may be used to determine aquifer dynamics or used in combination with dissolved and free gas compositional analysis to determine accurately gas ratios for water age dating and other computations.

The described instrument was useful in examining the development of excess air in groundwater. Excess air (Heaton & Vogel 1981; Aeschbach-Hertig et al. 2000; Klump et al. 2008; Solomon et al. 2011) in groundwater was formed either by fluctuating water levels at the recharge pressurizing gas in the pore space or through vorticity in rapidly descending waters in fractured or karstified formations. Dissolved gas analysis is commonly used to calculate temperature at recharge by assuming that the saturation level of atmogenic gas is temperature driven; however, excess air is shown as a pressure phenomenon related to the depth of free gas entrapment in porous media (Holocher et al. 2002; Jung & Aeschbach 2018). By measuring ebullated gas, gas flux, and dissolved phase gas concentrations, the total gas saturation per unit mass of the discharge water (hydropneumograph) can be obtained and used to evaluate the likelihood of a temperature or a pressure driving force for the excess dissolved gas.

CHAPTER IV

RESULTS

Improving Gas-Derived Aquifer Parameters Using Free-Phase Gas Measurements

Article Submission: Preparing Manuscript for Groundwater

Authors: Robert J. Agnew, and Todd Halihan

Monitoring data from wells and discharge data from springs provide significant insights into aquifer dynamics. However, the quantitative physical migration of the free gas phase, when present, has sparing representation in the transport literature aside from effervescing (Type IV) springs (Agnew and Halihan 2018). Numerous groundwater springs have multiphase flow (Agnew and Halihan 2018), but current literature regarding springs that have free gas phase bubbles present (Type III), that are not effervescent, is sparse. How researchers approach free-phase gas chemical analysis in these springs is unknown, but it may be assumed that most generally ignore free gas phase effects, likely assuming that the ratio of He/Ne is largely unaffected by free phase gas (bubbles) and

consider the ratio to be between 0.220 and 0.288 (Aeschbach-Hertig, Peeters, et al. 2000). Parameters of importance for groundwater aquifers, recharge temperature and apparent age, are dependent upon the accurate determination of the dissolved gas content of the recharge waters ((Schlosser, et al. 1989) (Stute and Schlosser 1993) (Aeschbach-Hertig, Peeters, et al. 2000) and others). Failure to consider the free gas phase may result in errors in determination of recharge temperature and other parameters collected using these data, particularly in karst aquifers where multiphase flow is common.

Significant work has been performed sampling and modeling gas transport in groundwater, beginning with the amount of atmogenic gas in equilibrium with water, or Air Equilibrated Water (AEW) (R. F. Weiss 1970) (R. F. Weiss 1971) (Weiss and Kyser 1978) (Clever 1979). Groundwater typically contains greater abundance of dissolved atmogenic gasses than AEW. This over-abundance of dissolved gas, or "Excess Air" (Herzberg and Mazor 1979), (Heaton and Vogel 1981) is driven by surface tension and capillary effects (Klump, et al. 2007) and water table fluctuations (Aeschbach-Hertig, Peeters, et al. 2000). These mechanisms for the development of excess air have been confirmed in a laboratory column experimental (Holocher, et al. 2002) and using an in-situ field experiment (Klump, et al. 2007).

By using the dissolved noble gas concentrations and Excess Air models, the temperature during recharge may be estimated, providing the Noble Gas Temperature (NGT) (Stute, et al. 1995) (Aeschbach-Hertig, Peeters, et al. 2000). The NGT is determined based upon the temperature dependence of the solubility of the noble gasses (R. F. Weiss 1970), (R. F. Weiss 1971), (Clever 1979), (Stute and Schlosser 1993) while accounting for Excess Air. Additionally, the dissolved Tritium/^{3}He may be used to

determine the duration the waters have been in the aquifer, or apparent age (Schlosser, et al. 1989).

In order to estimate the NGT, an excess air model is needed. The typical models have many commonalities, starting with the use of Air Equilibrated Water (or Air Saturated Water) derived from by Weiss (1970) (1971) (1978) and Clever (1979). All common models assume the absence of gas fluxes, particularly ebullative flux. Granted, diffusive flux occurs across the interfacial area (air/water surface at the discharge), past the point of underwater sampling, therefore ignoring diffusive flux is reasonable. These excess air models are solved using a computational inversion technique, (Sun, Hall and Castro 2010) (Jung and Aeschbach 2018). Caution must be used in the interpretation of these modeling results; Sun et al. (2010) shows statistically models can routinely get low Chi Square values due to inflation of original excess air concentration (A) before fractionation. Additionally, Cey et al. (2008), (2009) argue that goodness of fit is not a robust indicator of the appropriateness of an NGT model. Therefore, modeling results must be compared to physical realities to determine robustness and applicability to a given water system. For a thorough treatment of noble gas chemistry in natural waters see Kipfer et al. (2002).

While the typical excess air models have many commonalties, every model relies on specific assumptions in the computation of excess air. The Unfractionated Excess Air (UA Model) simply adds additional air of the composition of AEW to most closely reflect the measured concentrations of the gasses in the water sample (Andrews and Lee 1979); (Heaton and Vogel 1981); (Stute and Schlosser 1993). The Partial Re-equilibration (PR model) considers diffusive loss of some portion of the excess air (Stute,

et al. 1995). The Closed-system Equilibration (CE model) fixes a volume of air trapped in bubbles per unit mass of water (Aeschbach-Hertig, Peeters, et al. 2000). The Oxygen Depletion (OD) model assumes that the increase in noble gas concentrations is proportional to the partial pressure increase from the consumption of oxygen by biological processes (Hall, et al. 2005), (Castro, et al. 2007). The Partial Degassing (PD model) is a modification of the PR model using diffusive loss rather than re-equilibration (Aeschbach-Hertig, El-Gamal, et al. 2008). The Gas diffusion relaxation (GR model) is a modification of the OD model using diffusion and a loss of air (Sun, Hall, et al. 2008). The governing equations for the six listed models (UA, PR, PD, OD, GR, and CE) are well described in Jung & Aeschbach (2018) and subsequent references.

These excess air models are used to determine the NGT by fitting excess air parameters to the dissolved noble gas concentrations and the temperature dependent gas solubility. This analysis relies upon the difference in the neon concentration in the water sample and AEW (ΔNe), as neon's solubility is governed by excess head and has nearly negligible temperature dependence (Aeschbach-Hertig, Peeters, et al. 2000) (Aeschbach-Hertig, et al. 2002) (Kipfer, et al. 2002). Helium is not used in this determination due to non-atmogenic sources of helium being present in groundwater.

The amount of excess air, the NGT, and ΔNe are also necessary parameters for the tritium/^{3}He Groundwater Age Model. The accurate selection of the excess air model is critical for determination of water age (Peeters, et al. 2002) using the groundwater-dating procedure developed by Schlosser (1989), which is suitable for the determination of apparent age in young waters. Note that, "The tritium/^{3}He age is an apparent age

which is affected by ^{3}He loss due to incomplete confinement in the groundwater body and by mixing." (Schlosser, et al. 1989, 245).

While the dissolved gasses in groundwater have received much attention, the free gas phase, however, is given less emphasis in hydrogeology unless a source of contamination is present wherein the free gas phase (bubbles) provides a transport mechanism for contaminant migration (Patoczka and Wilson 1984) (Vroblesky & Lorah, Prospecting for Zones of Contaminated Ground-Water Discharge to Streams Using Bottom-Sediment Gas Bubbles, 1991) (McLinn and Stolzenburg 2009). Additionally, free phase gas from groundwater is given more attention in water purification engineering literature (Scardina 2004) (Scardina and Edwards 2006) where water movement through filter beds made of sand causes dissolution of the gas. Since bubbles provide a mechanism for transportation of dissolved phase components, the presence of bubbles at a groundwater discharge indicates the potential for stripping noble gasses from the dissolved phase, altering measurements.

Gas migration from dissolved to free phase has significant effects on dissolved gas content (White, Hem and Waring 1963); (Baird, Bottomley and Taitz 1979); (Patoczka and Wilson 1984); (Lucchetti and Gray 1988); (Vroblesky & Lorah, Prospecting for Zones of Contaminated Ground-Water Discharge to Streams Using Bottom-Sediment Gas Bubbles, 1991) (Mariner, et al. 2003) (Lavenson, et al. 2016) (Daniel A. B., 2018). The dissolution mechanism of the excess air is from velocity effects around obstructions based on observations in the Ash Meadows Flow System (Thomas, et al. 2002) and in filter beds of sand (Scardina 2004) (Scardina and Edwards 2006). The increased velocity results in a pressure drop following Bernoulli's Principle and provides

the necessary initiation energy for degassing to form the characteristic bubbles of a Type III Spring (Agnew and Halihan 2018). This induced phase change combined with the dissolved gases' Henry's Air-Water Partitioning Coefficient (K_{aw}) and Diffusivities drives the noble gasses of interest out of the dissolved phase with helium migrating to the free phase fastest and xenon migrating the slowest (Holocher, et al. 2002).

In order to discuss gas issuing from groundwater, some clear terms are needed. Since groundwaters have excess air, they will re-equilibrate with the atmosphere upon eruption at the surface. This re-equilibration, or mass transfer, is the total gas flux. If the re-equilibration occurs with the presence of bubbles, the total gas flux is the sum of the diffusive flux and either the ebullative flux or the effervescent flux. Diffusive flux is the mass transfer of dissolved gas to the atmosphere by diffusivity across the bulk interfacial area of the liquid (water) (Daniel A. B., 2018). Ebullative flux is the liberation of bubbles typical from a mechanical, or velocity induced, pressure drop typical of a Type III Spring, Bernoulli mechanism (Agnew and Halihan 2018). Effervescent flux is the liberation of bubbles formed by supersaturation (>3 bar or "sparkling") (Agnew and Halihan 2018)) of the dissolved gas typical of a Type IV "Soda Spring" (Agnew and Halihan 2018). Ebullative vs Effervescent flux is easily determined because, "Effervescing water will continue to bubble (for a time) when removed from the spring, unlike Bernoulli (III) bubbles." (Agnew and Halihan 2018, 864).

Given the abundance of excess air in groundwater and the number of springs known to ebullate, one must ask that if the free gas phase is discounted in ebullating springs, does significant error occur in the estimation of recharge parameters (age and temperature) in groundwater? If error in the estimation of excess air may results in an

error in the determination of ΔNe, that would then lead to an underpredicted Nobel Gas Temperature (NGT) proportional to the difference between the He/Ne ratio in AEW and the sample. If the hypothesis is correct, the difference between the errors of He and Ne should be proportional to the difference in dimensionless Henry's Air-Water partitioning coefficient (K_{AW}) in He and Ne and therefore drive a proportional error in apparent age. This investigation will evaluate theoretical errors introduced in the calculation of recharge parameters using noble gas analysis when the effects of multiphase flow are ignored. The potential errors will be tested at the Nelson Spring Complex, OK that has previously been evaluated using existing techniques (Christenson, Hunt and Parkhurst 2009). Finally, we examine the rapid fluctuation in water table level in this karst aquifer as the driving mechanism for excess air in the system.

Study Area

In order to test the ebullition-stripping hypothesis, a study area that minimizes the variables in dissolved gas chemistry is preferred. Specifically, an aquifer that exhibits rapid fluctuations in elevation of the water table at the recharge that will drive gas into solution creating excess air is ideal. The aquifer should also be isothermal or near isothermal to avoid temperature induced solubility changes or degassing. Ideally, the system should have large homogenous lithology with a central located flowline to provide stable water chemistry coupled with a long-term well data and water chemistry data for comparison of results. The lithology should also contain structures conducive to rapid flow, such as fractures or conduits, to allow for velocity induced pressure effects.

Finally, the system must terminate at a discharge with observed ebullition, preferably a Bernoulli (Type III) Spring (Agnew and Halihan 2018).

For this study, we selected the Eastern Arbuckle-Simpson aquifer as it satisfies all of the necessary criteria for hypothesis testing. The EAS aquifer is a well-characterized and stable aquifer comprised of ~1000 meter thick karstic fractured dolomite (Fairchild, Hanson and Davis 1990), (Swinea 2008). The EAS aquifer has a groundwater model available testing potential flowlines (Christenson, Osborn, et al. 2011). The flowline of interest is in the center of the aquifer (Figure 7) and shows little chemical variability in

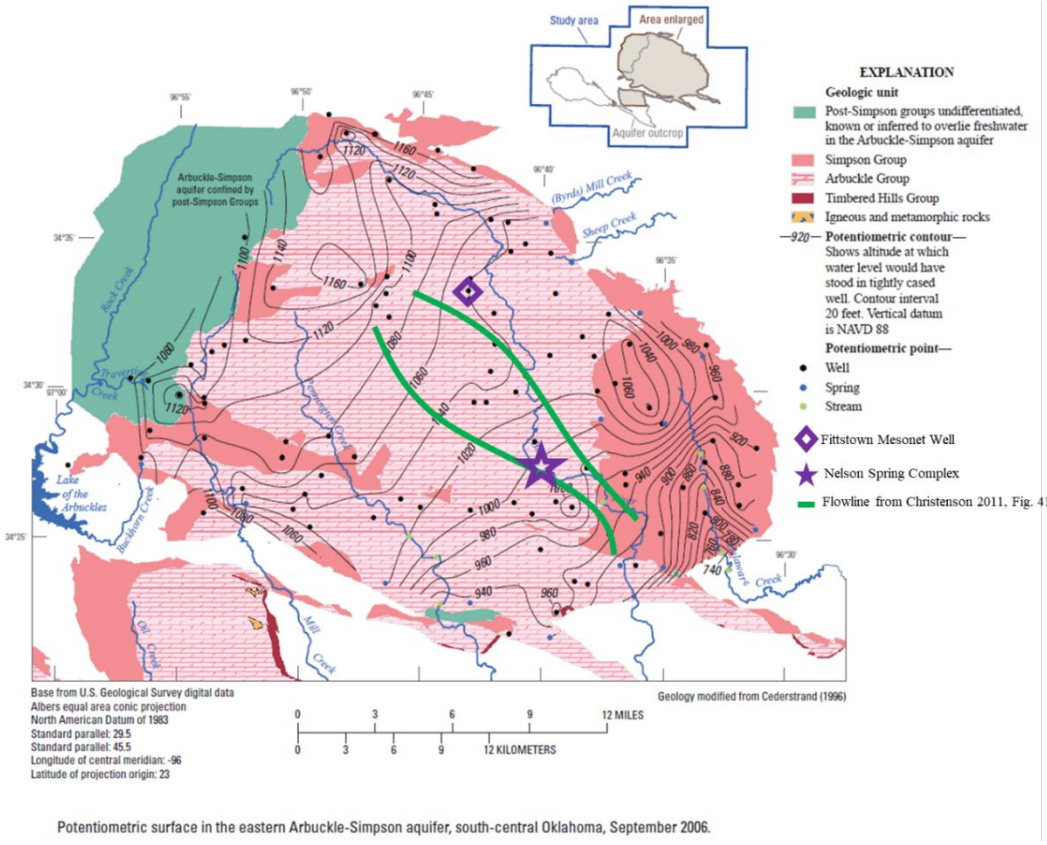

Figure 7. Arbuckle-Simpson Aquifer Potentiometric Surface and Flow Lines, After Christenson 2009, Fig. 20.

the groundwater (Christenson, Hunt and Parkhurst 2009). Most importantly, “The temperature data indicate that the aquifer is well connected vertically with flow processes nearly eliminating any geothermal gradient in the aquifer” (Halihan, Mouri and Pucket 2009, 1). The isothermal nature of the aquifer, less than 0.1 C variability as spring discharges in the Nelson Spring Complex (Swinea 2008) make the system ideal for dissolved gas chemistry investigations. Finally, across the EAS aquifer small karst features and regional faults are present (Christenson, Hunt and Parkhurst 2009) allowing for desired rapid flowpaths.

The recharge for the system is the Blue River Watershed extending ~12 miles to the NW of the spring (Christenson, Osborn, et al. 2011). The aquifer water table rapidly responds during rain events as indicated by the Fittstown Mesonet Well (no. 97451) located in the upper portion of the recharge seven miles northwest of the study spring (see Figure 7., green square on point). A recent record 36.80 cm of rain (14.49 inches) in 24 hours on 9/23/2018 resulted in a 12.5 meter (41 foot) increase in groundwater level in 4.17 days (See Figure 8. Fittstown Mesonet Well Plot) at the well (Oklahoma Water Resource Board 2005-2018). The average depth to groundwater is 28.7 m (94.1 ft) at the Fittstown Mesonet station (FITT) averaged over 5 years (2014-2018) at one-hour intervals. The RMS fluctuation of the aquifer mean water level, measured over the same period, is 5.71 meters (18.74 feet). The recharge temperature for the system is expected to be between 16.23 ˚C (mean annual temperature at FITT for 2004-2018) and 18.03 ˚C (precipitation-weighted mean temperature) (Mesonet 2019a).

The flowpath of interest for this study is located within the center of the formation outcrop area. The aquifer follows a potentiometric surface from 319 meters above mean

sea level (MAMSL) at the FITT to 305 MAMSL at the discharge 11.45 km away, resulting in a hydraulic gradient of 1:850, see Figure 7. (Adapted from (Christenson, Osborn, et al. 2011)). Karst features present in the outcrop imply the availability of rapid flowpaths. Additionally, test bores in the formation commonly encounter voids (Christenson, Hunt and Parkhurst 2009). Finally, fractures in the carbonate formation also allow for rapid water movement (Halihan, Mouri and Pucket 2009).

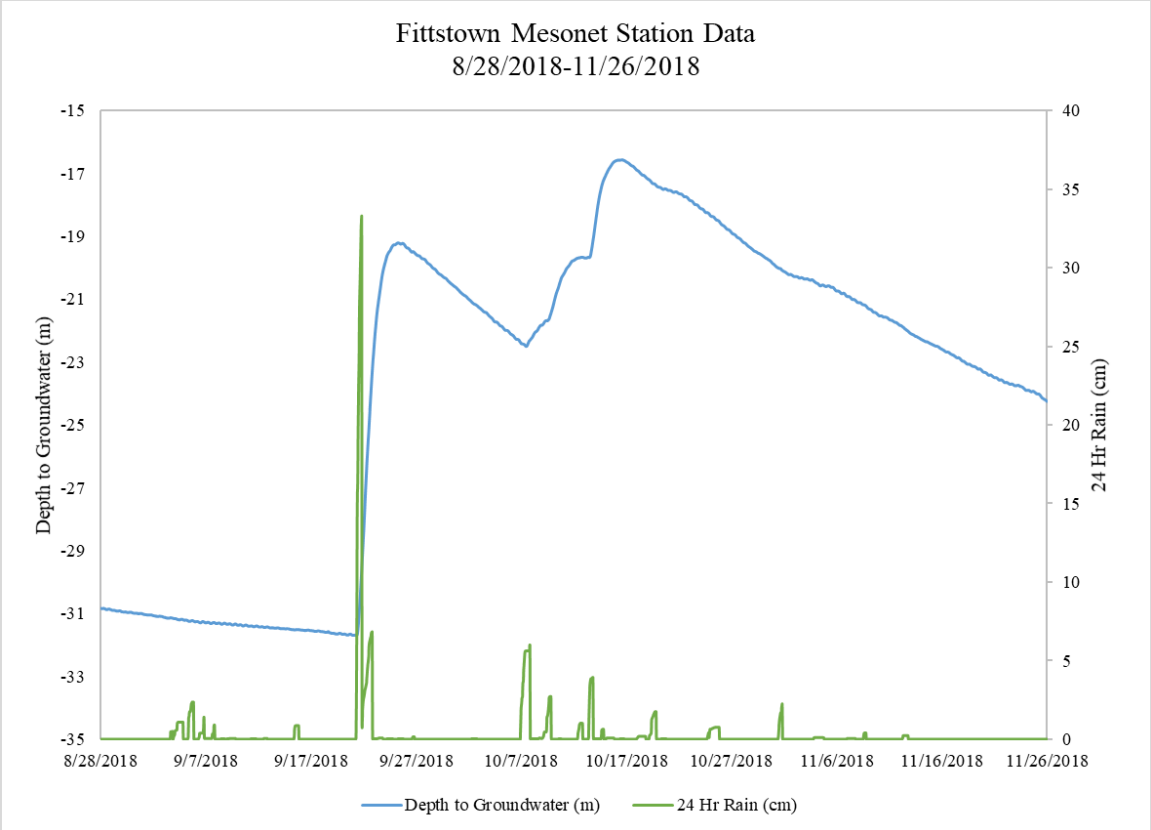

Figure 8. Fittstown Mesonet Well Log Rapid Recharge Event (Mesonet 2019)b.

The flowlines of interest intersect the surface to form numerous small springs along fracture traces. Excess head provides energy to drive a Bernoulli degassing process in the narrow fractures before the flowpath reaches the discharge creating Bernoulli (Type III) bubbles (Agnew and Halihan 2018). The specific discharge location is in the Nelson Spring Complex (Christenson, Hunt and Parkhurst 2009). The spring complex is located on the Arbuckle-Simpson ranch situated along the Blue River. A fifth magnitude spring within the complex named The Little Bubbler located at 34°27'26.23"N, 96°40'6.36"W was selected for its size and elevated position above the surrounding tributaries and for its nearly steady flow of gas (bubbles).

Methods

In order to measure and model gas migration, we obtain field data in the recharge zone to evaluate gas recharge. At the discharge site, an instrument that measures the flow of water and free phase gas from the study spring is described. Using dissolved and free phase gas measurements in combination with the flow measurements, we combine the results into a hydropneumograph. The values of total noble gasses in free and dissolved phases are used to model excess air, recharge temperature, and apparent age.

Recharge zone field data were collected at the Fittstown Mesonet Station and Fittstown Well (FITT), maintained by a partnership between the Oklahoma Mesonet and the Oklahoma Water Resources Board. The FITT collects an abundance of meteorological data; of interest to this study are air temperature, 24-hour rain totals, and depth to groundwater. The FITT is located 10 k. (6.3 mi.) SW of the town of Fittstown, OK in Pontotoc County Lat/Long: 34.552050° N, -96.717790° W. Well data from the

FITT was used to calculate the RMS flux of the groundwater surface from 2014 to present.

Spring gas and water data were collected using a hydropneumometer (Agnew & Halihan (Accepted on 3/2/2019). The instrument deployed from December 20, 2017 to August 7, 2018. The period reviewed in this study is February 4-7, 2018 when the dissolved and free gas samples were collected. Water flow was recorded using a standard weir per ASTM D5242-2013 (ASTM 2013) coupled with a pressure transducer and barometer. Free phase gas flow was recorded using a thermal mass flow meter (TMFM) connected to a capture shroud over the spring discharge. Local air temperature, barometric pressure, electrical conductivity (EC), and water temperature were also measured.

Compositional measures for the dissolved and free phase gasses were collected using the copper tube method as described by the USGS instructions for $^{3}H/^{3}He$ Noble Gas Sampling based on (Schlosser, et al. 1989). The copper tube apparatus was submerged in the pool created by the spring discharge using caution to prevent the formation of gas bubbles in the sampler. For the gas samples, the copper tube was connected to the discharge of the TMFM and allowed to purge prior to closure. The collection shroud was allowed to purge for 40 days prior to sample collection. The gas samples were analyzed by the USGS at the Geology, Geophysics, and Geochemistry Science Center using Techniques and Methods 5-A11 (Hunt 2015). Three repeat samples were collected for each phase (6 samples total), however, only one water sample and two free gas samples passed QA/QC.

The results of the gas analysis cannot be directly compared as the quantity of gas in water reported as ccSTP/g (H_2O) and free phase gas is reported as ccSTP/cc (where the volume fraction = mol fraction). Using the volumetric flow rates of the water and bulk gas the following procedure for combining dissolved and free phase results was used. Free phase gas flow rate ccSTP/sec multiplied by the reported mol fraction yields ccSTP/sec by species. Water flow rate in g/sec multiplied by gas species specific volumetric flow rate is normalized vs water to yield ccSTP/g(H_2O). Having both the free and dissolved phase gas quantities in the same units allows for the addition of water and gas species specific quantities to yield total gas in ccSTP/g(H_2O), see *Equation 6*

$$C_i^{g+w} = \frac{(C_i^g)(Q_g)}{Q_w} + C_i^w \qquad (6$$

Where:

C_i^{g+w} = Combined free and dissolved phase concentration of the i^{th} gas species in water (ccSTP/gH_2O)

C_i^g = Concentration of the i^{th} gas species in the free gas phase (ccSTP/cc)

Q_g = Total volumetric flow rate of the gas phase (ccSTP/s)

Q_w = Volumetric flow rate of the bulk liquid (water) (g/sec)

C_i^w = Concentration of the i^{th} gas species dissolved in water (ccSTP/gH_2O)

The species-specific noble gas concentration results were used to model the aquifer's recharge conditions. Aquifer recharge conditions, excess air and NGT, were

modeled using the PANGA software (Jung & Aeschbach (2018)) which expands the number of models available from the previous NOBLE software (Peeters, et al. 2002). The software fits noble gas parameters using an inversion technique described by McGrail (2001) that returns a Chi square value that is a minimization of the error-weighted square sum of the deviation about the measured and modeled noble gas concentrations (Jung and Aeschbach 2018). Field measurements of the discharge free-phase gas showed diminished oxygen concentration, indicating that the Oxygen Depletion (OD) model would be the most appropriate model for use with these data, and was therefore used for the study.

Additionally, the USGS dissolved gas analysis was used to estimate *apparent age* using the procedure from Schlosser, et al. (1989). The term apparent age is preferred because the calculation is susceptible to error from the vertical flux of gas due to poor confinement as well as other uncertainties in measurement. For apparent age modeling, the selection of the excess air model is critical for the accurate determination of water age (Peeters, et al. 2002) as recharge temperature and excess air fraction alter the computation by a "factor of 2." (Peeters, et al. 2002, 597).

Results

We present the results of the field data collection and the laboratory chemical analysis. These data include the physical measures taken at the study spring, the chemical analyses of the water and gas samples, and the modeling results for recharge temperature and apparent age. We additionally include our process for model selection and verification. Finally, we include a check of water table fluctuation vs the excess pressure predicted in the OD modeling results.

During the study period, the average water flow rate of the Little Bubbler Spring was 1.78E-03 m^3/sec with a range of 3.61E-04 to 4.07E-03 /sec, and a standard deviation of 0.63. The free-phase gas flow rate captured by the shroud was 5.51 ccSTP/sec, with a range of 4.27 to 7.3 ccSTP/sec, and a standard deviation of 0.26 ccSTP/sec. The average air temperature was 0.87 ˚C with a range of -10.2 to 18.19 ˚C, and a standard deviation 6.23 ˚C. In contrast, the average water discharge temperature was 16.0 ˚C, with a range of 15.1 to 17.56 ˚C, and a standard deviation of 0.56 ˚C. The variability of the discharge temperature is due to atmospheric influence on the spring pool used to seal the gas capture shroud. During the sampling period, the average barometric pressure was 972 mbar with a range of 871 to 1045 mbar, and a standard deviation 46.6 mbar. The average electrical conductivity (EC) was 579 µS/cm, with a range of 556 to 610 µS/cm, standard deviation 12.63 µS/cm. The physical parameter measurements are summarized in Figure 9. Hydropneumograph of the Little Bubbler Spring.

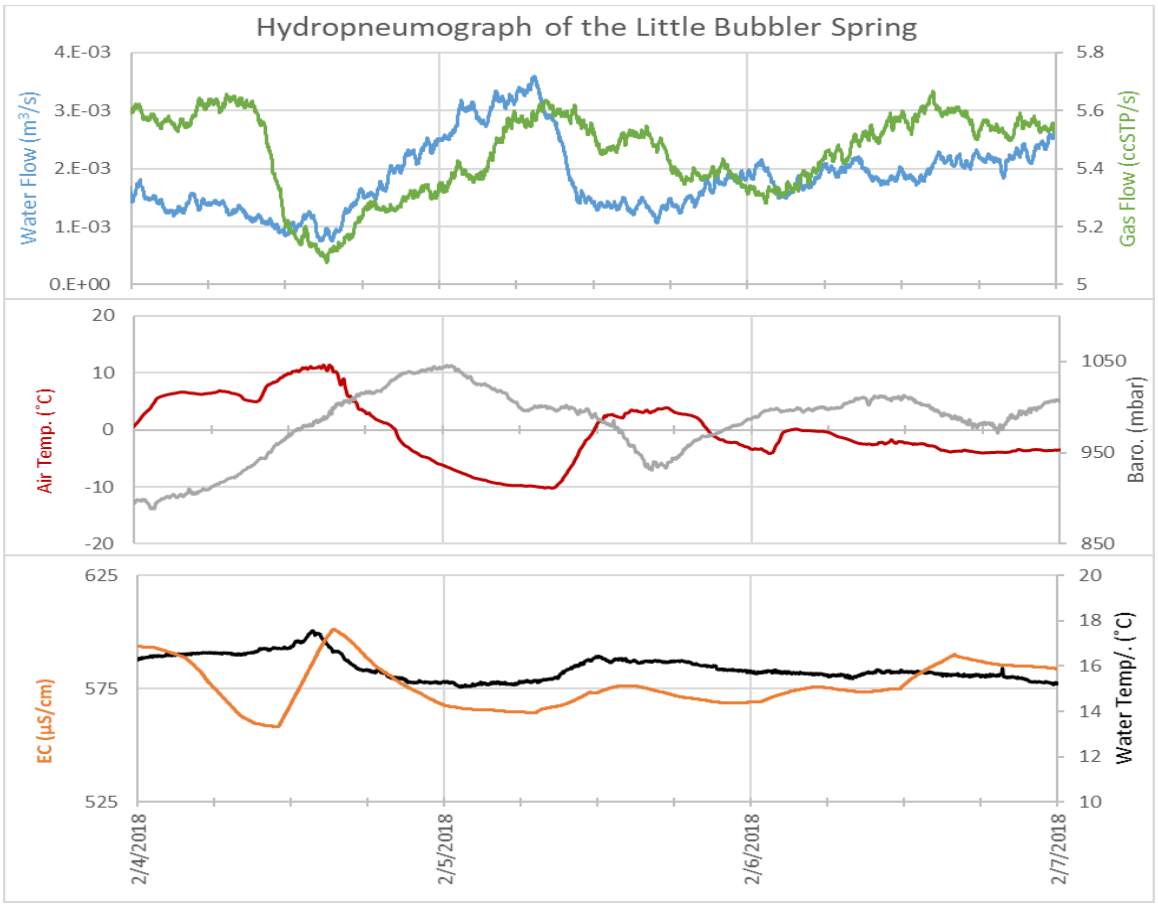

Figure 9. Hydropneumograph of the Little Bubbler Spring.

The compositional analysis of the free and dissolved gas phases included the five typical noble gasses and nitrogen. The free phase analysis also included oxygen and carbon dioxide. The water sample was also analyzed for tritium and ^{3}He for age dating. The results from the laboratory analysis for both the free and dissolved phase are presented in Table 4. USGS Compositional Results along with the combined value for total gas in ccSTP/gH_2O. A noticeable trend is observed of increasing error between the inclusion and exclusion of the free phase results from the heavy to light noble gases. The change in isotopic ratios, when considering the free and dissolved phase gas content, is

presented in Table 5. The change in the isotopic ratios is relatively small. However, a change in R/Ra will affect age dating calculations. The largest isotopic ratio difference of 4.4% was in the $^{20}Ne/^{22}Ne$ ratio and is important for model selection.

Table 4. USGS Compositional Results

Species	ccSTP/g(H2O)			%Error
	Water	Gas	Gas+Water	W vs W+G
He	1.03E-07	2.29E-08	1.27E-07	-18.7%
+/-	7.66E-10	2.29E-10	1.00E-09	
Ne	3.19E-07	6.06E-08	3.82E-07	-16.4%
+/-	6.38E-09	1.21E-09	7.64E-09	
Ar	4.38E-04	3.00E-05	4.70E-04	-6.6%
+/-	8.77E-06	1.50E-06	1.03E-05	
Kr	9.17E-08	3.35E-09	9.51E-08	-3.6%
+/-	2.75E-09	1.68E-10	2.92E-09	
Xe	1.27E-08	2.51E-10	1.29E-08	-2.0%
+/-	3.80E-10	1.26E-11	3.93E-10	
N2	2.30E-02	2.52E-03	2.56E-02	-10.2%
+/-	1.15E-03	5.99E-05	1.21E-03	

Table 5. USGS Ratio Results

Ratio	Water	Gas	Est. W+G	%Diff. W vs. W+G
R/Ra	0.954	0.976	0.957	2.3%
+/-	0.015	0.007	0.015	
$^{20}Ne/^{22}Ne$	9.825	10.273	9.857	4.4%
+/-	0.040	0.389	0.042	
$^{21}Ne/^{22}Ne$	NR	0.030	N/A	N/A
+/-	NR	0.002	N/A	
$^{40}Ar/^{36}Ar$	295.5	296.2	296.4	0.3%
+/-	1.341	5.924	1.359	
$^{38}Ar/^{36}Ar$	NR	0.188	0.000	N/A
+/-	NR	0.013	0.000	
$^{86}Kr/^{84}Kr$	0.304	0.305	0.305	0.1%
+/-	0.001	0.001	0.001	
$^{130}Xe/^{132}Xe$	0.148	0.151	0.149	1.4%
+/-	0.005	0.002	0.005	

Table 6. PANGA Modeling Results

Without Helium, Constrained

Model	*Chi Square*		*A [ccSTP/g]*		*T [˚C]*		*P_O*	
	W	*W+G*	*W*	*W+G*	*W*	*W+G*	*W*	*W+G*
OD	**0.58**	**0.59**	**1.69E-03**	**1.94E-03**	**16.76**	**17.39**	**1.20**	**1.22**
GR	Err	Err	Err	Err	Err	Err	Err	Err
CE	0.32	0.24	1.38E-02	1.63E-02	12.05	12.35	N/A	N/A
PD	0.24	0.22	5.48E-03	5.77E-03	11.88	12.17	N/A	N/A
PR	0.24	0.24	8.79E-03	1.24E-02	11.88	12.17	N/A	N/A
UA	1.61	1.50	7.09E-03	1.06E-02	10.93	11.22	N/A	N/A

Given the numerous excess air models available for the determination of the NGT, model selection is important to ensure accurate results. The gas sample analysis

shows an oxygen content of 11.8% (typical of groundwater (Tan 2000)). This value is consistent with gas-sample field measurements. Therefore, the Oxygen Depletion (OD) model is appropriate, assuming the oxygen depletion occurred at the recharge due to biological action (root respiration, decomposition of organic material, etc.) (Stute and Schlosser 1993). However, biological consumption of O_2 should produce an equimolar amount of CO_2 and the net partial pressure of the dissolved gasses should remain constant (Stute and Schlosser 1993). The gas sample indicates only 2.6% CO_2, which does not account for the ~10% reduction in oxygen. This mass imbalance is explained by the reactions of highly soluble CO_2 with the carbonate minerals (Drever 1997) of the Arbuckle group.

Since the OD model presumes that the depletion of oxygen causes the increase in partial pressures of the other dissolved atmogenic gasses, consideration must be given to an inverse scenario where an increase in another gas causes a proportion decrease in the abundance of oxygen, such as the production of nitrogen through the process of denitrification. Even considering that the nitrogen content of the discharging free-phase gas is 84%, for the EAS aquifer, denitrification is not likely. While excess of nitrogen is known to occur from denitrification (Musgrove, et al. 2016) (Böhlke, et al. 2009) (Addy, et al. 2002), the recharge area lacks the types of agriculture associated with nitrates. Additionally, four reductase steps are necessary to convert NO_3^- to N_2, which typically occurs in anoxic environments. The discharge water contains 12% oxygen and only 0.76 mg/L of nitrate as N and <0.008 mg/L as nitrite as N. Therefore, production of $NO \rightarrow N_2O \rightarrow N_2$ is unlikely and a mass balance of nitrate to N_2 would account for <0.5% of discharging gas. The excess N_2 is accounted for by depletion of O_2.

For this system, the OD model is an acceptable choice, but the other models should be given consideration. When examining the PR, CE, and UA models, the $^{20}Ne/^{22}Ne$ ratio best for determining model fits (Peeters, et al. 2002). The $^{20}Ne/^{22}Ne$ ratio in atmosphere is 9.80 (Ojima and Podosek 1983), and 9.78 in AEW (Beyerle, et al. 2000), from the same sources the $^{36}Ar/^{40}Ar$ ratio in the atmosphere is 296.0 and 295.93 in AEW. Because, "$^{20}Ne/^{22}Ne$ and $^{36}Ar/^{40}Ar$ in the gas excess should remain between the atmospheric ratio and the ratio at atmospheric solubility equilibrium if fractionation occurs according to the CE-model, but might be significantly smaller if the fractionation depends on the differences in molecular diffusivities (PR-model)" (Peeters, et al. 2002) and our data are 9.932 and 295.6 for gas+water (9.825 and 295.5 for water only), the PR model may be eliminated.

In using the PANGA software to model the excess air and NGT, all six models were run due to convenience even though the OD model was selected and the PR model eliminated. However, only the OD model returns a result that has a reasonable Chi square, a reasonable concentration of dissolved excess air in ccSTP/g H_2O, and most importantly a reasonable estimated recharge temperature between the mean annual temperature and the precipitation-weighted mean temperature. While the OD model is the most reasonable, it returns a P_{OD} that may appear be too high; this is addressed later in the water table fluctuations section. The results of the PANGA modeling are presented in Table 6 for all six models. The results are presented when running the model with only the dissolved gas analytical results (water only or "w" in the table) and when running the model with the dissolved plus free-phase gas analytical results (water+gas or "g+w" in the table.

For the OD model, the water only (dissolved gas) analysis returns a NGT of 16.8 ˚C whereas the water+gas (dissolved plus free phase) returns an NGT of 17.4 ˚C. The percent error between the gas and gas+water results is 3.4%, which, as predicted, roughly corresponds to the percent difference in the He/Ne ratios of gas vs gas+water of 2.8%. These parameters were then used in the apparent age modeling results. The apparent age of the water only portion of the gas is 10.5 years. The apparent age of the water plus free phase gas is 12.7 years. The percent difference in the apparent age of 17.3% roughly corresponds with the percent difference in the K_{AW} of He and Ne of 14.3%. Crucially, the revised temperature estimate of 17.4 ˚C lies between the expected values of 16.23 ˚C and 18.03 ˚C.

This modeling updates the values reported by Christenson et al. (2009) for recharge temperature and age for the spring discharges of the Nelson spring complex from 14.4 ˚C and 43.6 years apparent age to 17.4 ˚C and 12.7 years apparent age. These updated values decrease the apparent age by 71% and increase the temperature by 21%. A re-analysis of the 2009 Christenson et al. noble gas data using the OD model returns an estimated recharge temperature of 16.3 ˚C, similar to the 16.8 ˚C water only result in this study. These results are summarized in Table 7.

Table 7. Summary of Error Estimates Between Single Phase and Two Phase Estimates of Recharge Temperature and Apparent Groundwater Age (left 3 column), and comparison of Two Phase Estimates Compared to Previous Work (right 3 columns)

Parameter	W	W+G	%Diff.		C. 2009	A. 2019	%Diff.
ΔNe	175%	211%	-17%		60%	211%	-72%
Temp. (C)	16.8	17.4	-3.4%		14.4	17.4	-17%
App. Age (yrs.)	10.4	11.9	-13%		43.6	11.9	266%

W - Water values only
W+G - Water plus gas values
C. 2009 - Christenson et al. 2009
A. 2019 - This research

Returning to the topic of P_{OD}, and the question if the P_{OD} values returned by the model are excessive, we examine the implication of these results. Assuming excess air is proportional to amplitude of water table fluctuations (Aeschbach-Hertig, et al. 2002), and if P_{OD} (pressure increase from oxygen depletion) is equivalent to assuming a recharge altitude for the aquifer that is lower than the true recharge altitude (Sun, Hall and Castro 2010), then we can infer that P_{OD} may also be equivalent to the average depth of equilibration of the entrapped air at the recharge, which should be related to the RMS value of the water table fluctuation. For this system, P_{OD} is then a measure of both excess hydrostatic pressure and partial pressure increase due to oxygen depletion.

In a system with oxygen depletion being the only mechanism of increased pressure, a P_{OD} of 1.208 would equate to 100% oxygen depletion due to the 20.8% abundance of oxygen in the moist air of the equilibration zone. The model results show a P_{OD} of 1.201 for water only and 1.216when considering the gas+water analysis, which results in a partial pressure greater than 100% oxygen depletion. Sampling results and field measurements are consistent with an oxygen concentration in the water of 11.8%, or

a 43.2% O_2 depletion, which equates to a P_{OD} of 1.0896 from true oxygen depletion alone. Subtracting this result from the model derived P_{OD} yields a P_{OD} from excess head of 1.112 and 1.126 for water and water+gas respectively. Taking a P_{OD} of 1.2076 as 1 atmosphere of excess head and proportioning the revised P_{OD} values yields an excess head of 0.539 atm and 0.607 atm for gas and gas+water respectively. Converting atm to meters of water yields 5.57 mH_2O (18.3 ftH_2O) and 6.28 mH_2O (20.6 ftH_2O) for water and water+gas respectively. The RMS fluctuation of the aquifer of 5.71 meters is similar to these estimated values and is approximately one-half the peak amplitude of 12.4 meters (41 feet).

We examine the amplitude of the water table because, "Under recharge conditions typical for many aquifers, the excess dissolved gases, expressed by the relative Ne excess ΔNe, is mainly determined by the hydrostatic pressure on the entrapped air. Thus, we suggest that ΔNe is essentially a measure of the amplitude of water table fluctuations in the recharge area" (Aeschbach-Hertig, et al. 2002, 174). Looking at the results for ΔNe in this system using the OD model, water only yields ΔNe of 175%, water plus gas yields a ΔNe of 211%. Therefore, ΔNe is under predicted by 35% in this system when ignoring the free-phase gas discharge.

Discussion

We show that error is in fact introduced into the estimation of recharge parameters (excess air, ΔNe, age, and temperature) if the free gas phase is ignored in ebullating springs. The error in the estimation of excess air driven by a 35% error in ΔNe which leads to a modest underprediction error in Nobel Gas Temperature (NGT) of 3.6%, similar to the difference in the He/Ne ratio. The difference between the errors of He and

Ne quantity are proportional to the difference in dimensionless Henry's Air-Water partitioning coefficient (K_{AW}) in He and Ne and therefore drive a proportional overprediction error of 17% in apparent age. Finally, we link the RMS flux of the water table at recharge to the quantity of excess air using the OD model.

Many authors have stated that ebullition may result in errors in dissolved gas analysis. However, the quantification of this error in natural systems, to our knowledge, has not been measured. For the spring in study, we show a >10% error in the total dissolved gas content and a >16% error in Ne species-specific error. As the transfer of air into water in the recharge (Holocher, et al. 2002) and the mass transfer to bubbles (Daniel A. B., 2018) near the discharge is governed by Henry's constant, then the expected difference in the concentration of dissolved gas between air equilibrated water and water with excess air should correspond with the Henry's Air-Water Partitioning Coefficient (K_{AW}). As a check of data validity, we shown that ignoring the mass of the exsolved gas introduces error proportional to the magnitude of K_{AW}, Figure 10. Therefore, we conclude that for ebullating springs, consideration of the free phase gas is essential in reducing errors in calculating recharge parameters and water age. The strong correlation between K_{AW} and our computed error ($R^2 = 0.9973$) is indicative of this method's ability to accurately measure total dissolved gas concentrations.

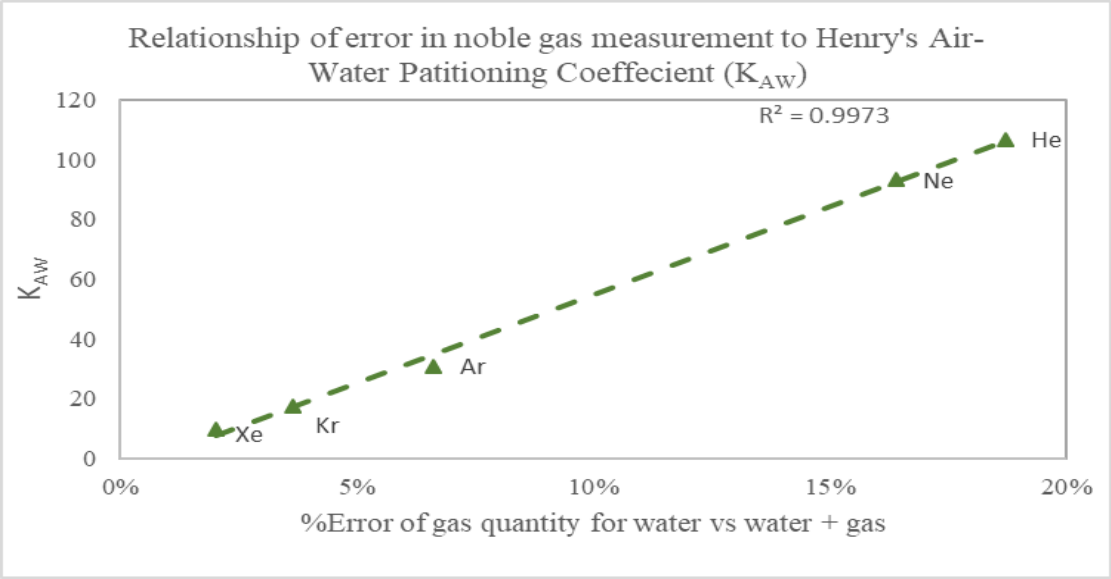

Figure 10. Relationship of Error in Noble Gas Measurement to Henry's Air-Water Partitioning Coefficient (K_{AW})

By examining the both the free and dissolved phases of atmogenic gasses in groundwater systems, a Multiphase Gas Transport Model may be conceptualized, see Figure 11. At the recharge, meteoric water equilibrates with the atmosphere (Air Saturated Water) (R. F. Weiss 1970) beginning the gas cycle. Additional air volume is added to the water through surface tension and capillary effects in the quasi-saturated zone (Klump, et al. 2007) as it infiltrates. During infiltration, a rapid rise in the groundwater surface traps air bubbles in the matrix and the water re-equilibrates with the trapped air generating "Excess Air" (Heaton and Vogel 1981). In the recharge zone of the aquifer, biological action may reduce the oxygen content of the groundwater and proportionally increase the partial pressure of the other dissolved gasses, with some

production of CO_2 (Stute and Schlosser 1993). The dissolved gasses are transported through the aquifer, with the possible reduction of CO_2 through carbonate mineralization (Christenson, Hunt and Parkhurst 2009). During migration across the aquifer, infiltration of helium may occur from the mantle and helium may also escape through incomplete confinement (Schlosser, et al. 1989). If there is sufficient hydrostatic head to accelerate water in a low resistance path (fracture or conduit), possibly past a flow restriction, increasing velocity and decreasing pressure, resulting in the degassing of the waters (Thomas, et al. 2002). If the degassing occurs near the spring discharge, then a Type III spring with Bernoulli bubbles (Agnew and Halihan 2018) is formed.

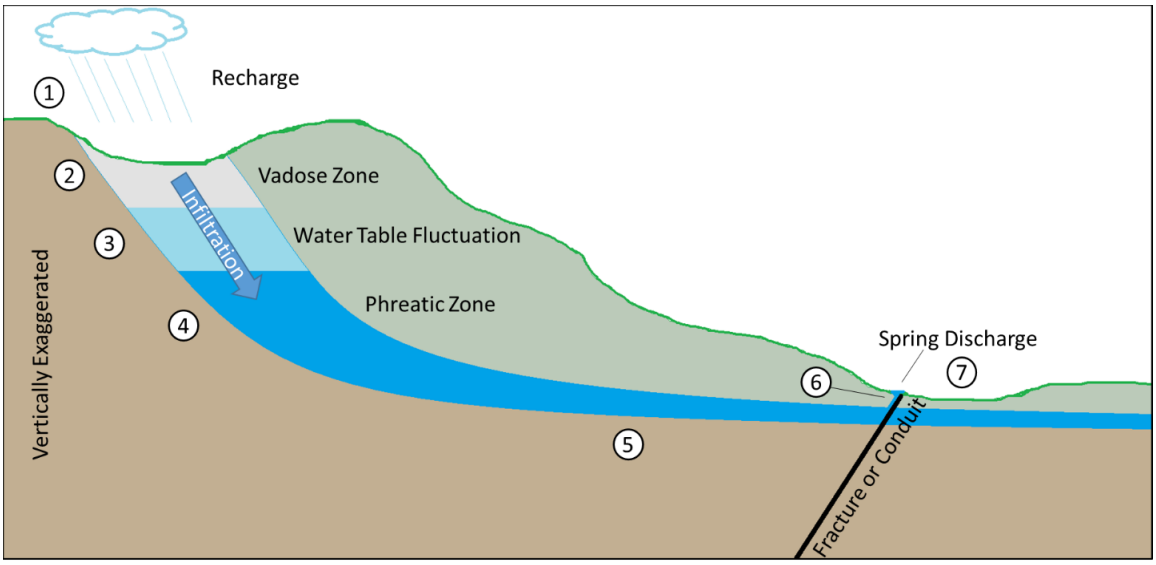

General Model	Arbuckle-Simpson Model
1. Meteoric water equilibrates with the atmosphere (Air Saturated Water) (Weiss 1970).	1. Meteoric water equilibrates with the atmosphere between 16.23 °C (mean annual temperature) and 18.03 °C (precipitation weighted mean temperature) (Mesonet 2019).
2. Additional air volume is added to the water through surface tension and capillary effects in the vadose zone (Klump et al. 2007).	2. Ibid.
3. A rapid rise the groundwater surface traps air bubbles in the matrix and the water re-equilibrates with the trapped air generating "Excess Air" (Heaton & Vogel 1981).	3. Excess air from water table RMS flux between 2014-2018 of 5.71 m, peak amplitude of 12.4 m (Mesonet 2019).
4. Biological action reduces oxygen content of the groundwater and proportionally increases the partial pressure of the other dissolved gasses, with some production of CO_2 (Stute & Schlosser 1993).	4. Oxygen content of discharge of 11.8%.
5. Transportation of dissolved gas through the aquifer. Reduction of CO_2 through carbonate mineralization (Drever 1997). Infiltration of helium may occur from the mantle, helium may also escape through incomplete confinement (Schlosser et al. 1989).	5. CO_2 content of discharge of 2.6% (not equimolar with 8.9% decrease in oxygen, consistent with carbonate interaction).
6. Aquifer hydrostatic head accelerates water in a low resistance path (fracture or conduit) past a flow restriction, increasing velocity and decreasing pressure, resulting in the degassing of the waters (Thomas et al. 2002).	6. ~10% of the total gas (N_2) lost to ebullition.
7. Bernoulli (Type III) multiphase spring discharge with bubbles (Agnew & Halihan 2018).	7. Estimated recharge temperature of 17.4 °C and apparent age of 12.7 years.

Figure 11. Multiphase Gas Transport Model.

While this work gives an end-to-end treatment of multiphase gas flow in aquifers, the results have limitations. Additional work is needed in the characterization of the free gas component for ebullating springs. This initial study provides only a limited sample size on one small spring, making additional confirmation necessary to see if the results are consistent among multiple groundwater systems and spring magnitudes.

In the future, we hope to deploy a real-time multiphase analyzer using a permanent capture structure collecting data over several recharge cycles. This longer-term study would be necessary to begin to solidify the relationship between ebullition and dissolved gas content in detail. By coupling real-time dissolved and free gas measurement with traditional laboratory analysis, a more complete picture of how apparent age and recharge temperature measurements are altered throughout the recharge cycle can be obtained.

Conclusions

Use of dissolved noble gasses to estimate recharge parameters of temperature and age are well-established (Stute, et al. 1995) (Aeschbach-Hertig, Peeters, et al. 2000). Further, the action of bubbles to strip dissolved gasses is well-established (White, Hem and Waring 1963); (Baird, Bottomley and Taitz 1979); (Patoczka and Wilson 1984); (Lucchetti and Gray 1988); (Vroblesky & Lorah, Prospecting for Zones of Contaminated Ground-Water Discharge to Streams Using Bottom-Sediment Gas Bubbles, 1991) (Mariner, et al. 2003); (Lavenson, et al. 2016); (Daniel A. B., 2018). However, the literature, to our review, is largely void of reports on the presence of bubbles at springs where dissolved gas data is collected and then analyzed. We quantify the error in dissolved gas analysis in a bubbling spring and show the error is proportional to known

physical principles of the Henry Air-Water Partitioning Coefficient and the formation of excess air related to the RMS flux of the water table at the recharge. This result from a single spring needs to be expanded to determine if the relationships identified hold across scales and from bubbling springs of different geology. Extending the work of many other researchers, we show a more complete multiphase gas cycle in Type III springs. This more complete multiphase gas cycle in conjunction with the associated errors in dissolved gas analysis, particularly derived recharge temperature and subsequent apparent age, indicates a re-analysis of these estimates for certain aquifers that exhibit ebullition at the discharge.

CHAPTER V

CONCLUSION

This work examined questions related to errors associated with predictions of aquifer parameters based upon dissolved gas measurements in bubbling springs. Specifically, does the presence of bubbles at a spring introduce errors into the estimation of total gas content in the waters and if so, by how much? Does the measured error match the expected error based upon our knowledge of first principles? Does the error in the estimation of total gas content affect the estimation of excess air at the recharge, and if so how much? How does the error in excess air affect the estimation of recharge temperature? Finally, how does the error in the estimation of excess air and recharge temperature affect the estimation of groundwater age?

As predicted, this work shows that error is in fact introduced into the estimation of recharge parameters (age and temperature) if the free gas phase is ignored in ebullating springs. The error in the estimation of excess air is driven by a 33% error in changes in Neon that leads to a modest error in predicted Nobel Gas Temperature (NGT) of nearly 2%, proportional to the predicted difference from the proportionality of the He/Ne ratio. The difference between the errors of He and Ne quantity are proportional to the

difference in dimensionless Henry's Air-Water partitioning coefficient (K_{AW}) in He and Ne and therefore drive a proportional error of 17% in the estimation of apparent age.

Therefore, the hypothesis that ignoring the free gas phase in bubbling springs results in the introduction of errors in the estimation of recharge parameters is confirmed. The introduced error is governed by the physical parameters of the He/Ne ratio and K_{AW}, which lends validity to the work and provides a basis to establish correction methodology for these errors.

Discussion

Interpretation of Results

Applying the results of this work specifically to the Nelson Spring Complex demonstrates the importance in accurately measuring total gas content among all phases. Inaccurate determination of excess air may result in improper excess air model which then compounds to the predicted noble gas temperature, and further to the estimation of apparent age. This work updates the values reported by Christenson et al. (2009) for recharge temperature and age for the spring discharges of the Nelson spring complex from 14.4 ˚C and 43.6 years apparent age to 16.8 ˚C and 12.7 years apparent age. By re-analyzing the Christenson et al. (2009) noble gas data using the Oxygen Depletion (OD) model, rather than the previously used Closed Equilibrium (CE) model, returns an estimated recharge temperature of 16.3 ˚C (without including free gas) which then shows consistency within the known isothermal aquifer across an 11 year span between sampling events.

Limitations of the Research

Additional work is needed in the characterization of the free gas component for ebullating springs. This initial study provides only an extremely limited sample size on one small spring, making these findings preliminary. This work also was undertaken on a karst spring characterized by Type III bubbles. Transferability of these results to non-karst or non-Type III bubbling springs needs further evaluation.

Contributions to Knowledge

This work expands understanding of gas in groundwater on several fronts. First, seven bubble facies are provided to organize and foster lines of research based on specific mechanisms of gasification and degasification of groundwater. Next, this work provides a field method for capturing and measuring free gas flow from bubbling springs. This device allows for both the determination of total dissolved gas content as well as provides a new tool for the understanding of aquifer dynamics, the hydropneumograph. The hydropneumograph shows promise in expanding our understanding of flow dynamics within aquifers. Finally, the improved determination of total gas content allows for quantification of the errors in the estimation of excess air, recharge temperature, and apparent age. In combination, better estimation of recharge temperature and age allows for an improvement in the reconstruction of paleoclimate.

Key Contributions of this work

- Systematic description of seven mechanisms, categorized as facies, for bubbling springs
- Cost effective method for collecting and computation of total gas discharge from bubbling springs
- Quantification the errors associated with dissolved gas analysis when the free gas phase is ignored, particularly for the change in the quantity of neon, noble gas temperature, and apparent groundwater age
- Provided the first quantified demonstration of the relationship between water table fluctuation and the quantity of excess air
- Updated the recharge temperature and apparent age of the Arbuckle-Simpson aquifer at the Nelson Spring Complex

Future Research

The results from the hydropneumograph developed in this work may have application in the prediction of drinking water quality in certain springs. Byrds Mill Spring, located 12 miles to the south of the City of Ada, OK is the primary drinking water source for the city's 17,400 residents (US Census Bureau, 2013). The spring water exhibits rapid decreases in electrical conductivity (EC) soon after large rain events. As this change in EC is indicative of water that has not been in prolonged contact with the rock matrix, and the surrounding recharge area is known to be karstified with sinkholes and other rapid flow features, this rainwater incursion may coincide with a decrease in

water quality in the spring waters. While EC may be an indication that lower quality water may have arrived at the intake for the city's water supply, the proposed method of using a hydropneumograph for predicting the event would allow time for intervention by providing a precursor for water quality changes.

Byrds Mill spring, as well as numerous other springs in the region, is observed to ebullate gas ~0.03 m^3/s. This work shows that at a nearby spring, the gas discharge rate increases 18-24 hours before the water flow rate increases. This increase in ebullition may act as an *a priori* indication of an incoming change in water quality.

At Byrds Mill Spring, numerous flowpaths are indicated by both water chemistry and electrical resistivity imaging (ERI). During base flow, the spring exhibits constant EC and temperature, while during surge flow, EC drops to near zero, while temperature stays nearly steady. The multiple flowpaths indicated by ERI are hypothesized to reflect a deep (>1km) flow path and a much shallower flowpath connected to surface dolines. This rapid connection to surface waters is further evidenced by the water table fluctuations measured at the Fittstown Mesonet Station 4 miles to the southwest of the spring. The water table shows drastic changes in response to precipitation, raising 40 feet in 4 days in September of 2018. By studying total gas composition at this spring, the regional groundwater model of the Arbuckle-Simpson Aquifer could be improved by providing a basis for the quantity of water flow from the deep (old) and shallow (young) flowpaths.

The goal is to expand on the previously developed method of determining a hydropneumograph for an ebullating spring by examining a major ebullating spring for several annual rain cycles. Additionally, by combining this method with the technique of field mass spectrometry by Brennwald (2016), it is hoped to establish a new benchmark

in the study of gas dynamics in springs with excess air (Heaton & Vogel, 1981), especially with sufficient excess air to induce ebullition. By doing so, periods of diminished water quality for the supply for the City of Ada may be predicted. This work may also enhance the existing groundwater model for the Arbuckle-Simpson aquifer, and provide for the hydrogeologist community a new technique for understanding water-gas dynamics.

In addition to measuring the quantity of the gas and liquid phase flows, measuring the composition of the atmogenic gasses in the dissolved in free phases is possible using a "miniRuedi" gas-equilibrium membrane-inlet mass spectrometer (GE-MIMS) as described in Brennwald et al. (2016) and available from Gasometrix. The GE-MIMS using a passive membrane sampler deployed in the water, which equilibrates with the dissolved gasses and provides means for analysis. The free gas collected by the spring box enclosure can be directly measured via a sampling tube in the discharge vent. The miniRuedi would provide quantification to the ppm level for He, Ar, Kr, N_2, O_2, CO_2, CH_4, and H_2 with an analytical uncertainty of 1-3%. This study would produce the first ever species-hydropneumograph. Based upon the team's research, to be included in a forthcoming publication on a nearby karst spring, the oxygen depletion (OD) model is best suited for the determination of recharge temperature from noble gas solubuilities. With the OD model, the concentrations of only three noble gasses are necessary to determine the system. Additionally, with the miniRuedi providing oxygen concentration, the OD model becomes over determined.

In addition to the miniRuedi instrument, periodic sampling of both the free and dissolved gas phases will be undertaken using the traditional copper tube method and

analyzed at the USGS Geology, Geophysics, and Geochemistry Science Center. These samples will serve as a touchstone for the continuous field measurements from the GE-MIMS as well as provide point data for Ne and Xe, as well as more detailed isotopic analysis necessary for age dating.

This proposed work has expected benefits related to local water quality, a regional benefit to improve the groundwater model, and broad goal to produce a new technique for the analysis of groundwater in ebullating springs. The tactical benefit is to provide the City of Ada with an a priori system to predict degrading water quality so that timely interventions can be made. Finally, this work will provide the first in-depth analysis of how ebullition impacts dissolved gas analysis allowing for improved estimation of recharge conditions and age. Additionally, we hope that by beginning this new line of hydrogeologic research, additional insights into groundwater mechanics may be revealed.

REFERENCES

Aalborg. (2016). Operating *Manual: XFM Digitial Mass Flow Meters.* Orangeburg, New York, NY: Aalborg. Retrieved from XFM Digital Mass Flow Meter Product Documentation: ttp://www.aalborg.com/images/file_to_download/en_Aalborg_EM20170915_XFM.pdf

Addy, K., Kellg, D Q, Gold, A.J., Groffman, P.M., Ferendo, G. and Sawyer, C. (2002). "In situ push-pull method to determine ground water denitrification in riparian zones." *Journal of Environmental Quality* 31 (3): 1017-1024.

Aeschbach-Hertig, W., El-Gamal, H., Wieser, M. and Palcsu, L (2008). "Modeling excess air and degassing in groundwater by equilibrium partitioning with a gas phase." *Water Resources Research* 44 (W08449): 1-12. doi:10.1029/2007WR006454.

Aeschbach-Hertig, W., Beyerle, U., Holocher, J., Peeters, F., and Kipfer, R. (2002). "Excess Air in Groundwater as a Potential Indicator of Past Environmental Changes." *Water Resources and Drinking Water* (Swiss Federal Institute of Environmental Science and Technology) 174-183.

Aeschbach-Hertig, W., Peeters, F., Beyerle, U. and Kipfer, R. (2000). Palaeotemperature reconstruction from noble gases in ground water taking into account equilibration with entrapped air. *Nature, 405*, 1040-1044.

Agnew, R.J. and Halihan, T. (Accepted on 3/2/2019). "An Instrument for the Determination of a Hydropneumograph in a Bubbling Spring." *Groundwater.*

Agnew, R. J. and Halihan, T. (2018). Why Springs Bubble: A Framework for Gas Discharge in Groundwater. *Ground Water*. doi:doi: 10.1111/gwat.12789

Alfaro, C. and Wallace, M. (1994). "Origin and classification of springs and historical review with current applications." *Environmental Geology* 24: 112-124.

American Geosciences Institute. (2016). "Glossary of Geology." *American Geosciences Institute.* http://www.americangeosciences.org/pubs/glossary.

American Industrial Hygiene Association. (1998). *The Occupational Environment - Its Evaluation and Control.* Edited by Salvatore R. DiNardi. Fairfax, VA: American Industrial Hygiene Association.

American Society for Testing and Materials (ASTM). (2013). *Standard Test Method for Open-Channel Flow Measurement of Water with Thin-Plate Weirs.* West Conshohocken, PA: ASTM.

Amos, R. T. and Mayer, K. U. (2006). "Investigating the role of gas bubble formation and entrapment in contaminated aquifers: Reactive transport modelling." *Journal of Contaminant Hydrology* 123-154.

Anderson, W. (1890). *Mineral springs and health resorts of California, with a complete chemical analysis of every important mineral water in the world.* San Francisco, CA: The Bancroft Company.

Andrews, J. N. and Lee, D. J. (1979). Inert gases in groundwater from the Bunter Sandstone of England as indicators of age and palaeoclimatic trends. *Journal of Hydrology, 41*, 233-252.

Aritomi, M., Kikura, H. and Suzuki, Y. (2000). Ultrasonic Doppler Method for Bubbly Flow Measurement. *4th Workshop on Measurement Technique for Stationary and Transient Two-Phase Flows*, (pp. 3-22). Rossendorf, Germany.

Atkins, T. and Escudier, M. (2013). *A Dictionary of Mechanical Engineering.* Oxford: Oxford University Press.

ASTM. (2013). *D5242-92 Standard Test Method for Open-Channel Flow Measurement of Water with Thin-Plate Weirs.* American Society for Testing and Materials Baird, R., Bottomley, J. and Taitz, H. (1979). Ammonia Toxicity and pH Control in Fish Toxicity Bioassays of Treated Wastewaters. *Water Research*, 181-184.

Bergfeld, D., Evans, W. C., Lowenstern, J. B. and Hurwitz, S. (2012). "Carbon dioxide and hydrogen sulfide degassing and cryptic thermal input to Brimstone Basin, Yellowstone National Park, Wyoming." *Chemical Geology* 233-243.

Bernoulli, D. (1968). *Hydrodynamica.* Translated by Thomas Carmody and Helmut Kobus. Argentorati (Strassburg): Dover Publication Company/Johann Reinhold Dulsecker.

Beyerle, U., Aeschbach-Hertig, W., Imboden, D.M., Baur, H., Graf, T. and Kipfer, R. (2000). "A Mass Spectrometric System for the Analysis of Noble Gases and Tritium from Water Samples." *Environmental Science Technology* 34 (10): 2042-2050. doi:10.1021/es990840h.

Blesson, L. (1832). "Observations on the Ignis Fatuus, or Will-with-the-Wisp, Falling Stars, and Thunder Storms." *Edinburg New Philosophical Journal* 90-94.

Bohlke, J. K., Antweiler, R. C., Harvey, J. W., Laursen, A. E., Smith, L. K., Smith, R. L. and Voytek, M. A. (2009). "Multi-scale measurements and modeling of denitrification in streams with varying flow and nitrate concentration in the upper Mississippi River basin, USA." *Biogeochemistry.* doi:0.1007/s10533-008-9282-8.

Bonacci, O. and Bojanić, D. (1991). Rhythmic Karst Springs. *Hydrological Sciences Journal*, 35-47.

Bräuer, K., Kämpf, H., Faber, E., Koch, U., Nitzsche, H. M. and Strauch, G. (2005). Seismically triggered microbial methane production relating to the Vogtland—NW Bohemia earthquake swarm period 2000, Central Europe. *Geochemical Journal, 39*, 441-450.Bräuer, K., Kämpf, H., Koch, U., & Strauch, G. (2011). Monthly monitoring of gas and isotope compositions in the free gas phase at degassing locations close to the Nový Kostel focal zone in the western Eger Rift¸ Czech Republic. *Chemical Geology*, 163-176.

Bräuer, K., Kämpf, H., Niedermann, S. and Strauch, G. (2013). "Indications for the existence of different magmatic reservoirs beneath the Eifel area (Germany): A multi-isotope (C, N, He, Ne, Ar) approach." *Chemical Geology* 356: 193-208.

Bräuer, K., Kämpf, H., Koch, U. and Strauch, G. (2011). "Monthly monitoring of gas and isotope compositions in the free gas phase at degassing locations close to the Nový Kostel focal zone in the western Eger Rift¸ Czech Republic." *Chemical Geology* 163-176.

Brennen, C. E. (2005). *Fundamentals of Multiphase Flows.* Cambridge, MA: Cambridge University Press.

Brennwald, M., Schmidt, M., Oser, J. and Kipfer, R. (2016). A Portable Autonomous Mass Spectrometric System for On-Site Environmental Gas Analysis. *Environmental Science & Technology*, 13455-13463.

Bryan, K. (1919). "Classification of Springs." *The Journal of Geology* 27 (7): 522-561.

Castro, M.C., Hall, C.M., Patriarche, D., Goblet, P. and Ellis, B.R. (2007). "A new noble gas paleoclimate record in Texas — Basic assumptions revisited." *Earth and Planetary Science Letters* 257: 170-187. doi:10.1016/j.epsl.2007.02.030.

Cey, B.D., Hudson, B.G., Morgan, J.E. and Scanlon, B.R. (2008). "Impact of Artificial Recharge on Dissolved Noble Gases in Groundwater in California." *Environmental Science Technology* 42 (4): 1017-1023. doi:10.1021/es0706044.

Cey, B.G., Hudson, B., Moran, J.E. and Scanlon, B.R. (2009). "Evaluation of Noble Gas Recharge Temperatures in a Shallow Unconfined Aquifer." *Groundwater* 47 (5): 646-659. doi:10.1111/j.1745-6584.2009.00562.x.

Chapelle, F. H., O'Neill, K., Bradley, P. M., Methé, B. A., Ciufo, S. A., Knobel, L. L. and Lovley, D. R. (2002). "A hydrogen-based subsurface microbial community dominated by methanogens." *Nature* 415: 312-315.

Christenson, S., Osborn, N.I., Neel, C.R., Faith, J.R., Blome, C.D., Puckette, J. and Pantea, M.P. (2011). *Hydrogeology and Simulation of Groundwater Flow in the Arbuckle-Simpson Aquifer, South-Central Oklahoma.* Reston, VA: 2011: U.S. Geological Survey.

Christenson, S., Hunt, A. G. and Parkhurst, D. L. (2009). *Geochemical Investigation of the Arbuckle-Simpson Aquifer, South-Central Oklahoma, 2004–06.* Reston, VA: USGS.

Clarke, T. (2001). "Taming Africa's killer lake." *Nature* 409: 554-555.

Clever, L. H. (1979). *Krypton, Xenon and Radon - Gas Solubilities - Solubility Data Series* (Vol. 2). (L. H. Clever, Ed.) New York, NY: Pergamon Press Inc.

Comas, X., Slater, L. and Reeve, A. (2008). "Seasonal geophysical monitoring of biogenic gases in a northern peatland: Implications for temporal and spatial variability in free phase gas production rates." *Journal of Geophysical Research.* doi:10.1029/2007JG000575.

Cook, C. W. (1870). "The Valley of the Upper Yellowstone." *Western Monthly Magazine* 60-67.

Council of the European Union. (1999). "On the Common Organisation of the Market in Wine." *Council Regulation No. 1493.*

Craig, H., Lupton, J. E., Welhan, J. A. and Poreda, R. (1978). "Helium isotope ratios in Yellowstone and Lassen Park volcanic gases." *Geophysical Research Letters.*

Craig, H., Boato, G. and White, D. E. (1956). "Isotopic geochemistry of thermal waters." *Proceedings of the 2nd Conference on Nuclear Processes in Geologic Settings.* National Academy of Science, National Research Council. 19-44.

CRC Press, Inc. (1987). *Handbook of Chemistry and Physics.* 68th. Edited by Robert C. Weast. Boca Raton, FL: CRC Press, Inc.

Crook, J. K. (1899). *The Mineral Waters of the United States and Their Therapeutic Uses.* New York, NY: Lea Brothers & Co.

Crossey, L. J, Karlstrom, K. E., Springer, A. E., Newell, D., Hilton, D. R. and Fischer, T. (2009). "Degassing of mantle-derived CO2 and He from springs in the southern Colorado Plateau region—Neotectonic connections and implications for groundwater systems." *Geological Society of America bulletin* 121 (7-8): 1034-1053.

Cunliffe, B. W. (1984). *Roman Bath Discovered.* Boston, MA: Routledge & K. Paul.

Czerski, H. and Deane, G. (2010). Contributions to the acoustic excitation of bubbles released from a nozzle. *The Journal of the Acoustical Society of America, 128*(5), 2625-2634.

Daniel, A. (2018). *Gas Evolution and Gas-Liquid Separator Modeling.* Stillwater, OK: Oklahoma State University.

Darcy, H. (2004). *Les Fontaines publiques de la ville de Dijon (The Public Fountains of the City of Dijon).* Translated by Patricia Bobeck. Dubuque, IA: Kendall Hunt Publishing Co.

Davis, S. N. and DeWiest, R. J .M. (1966). *Hydrogeology.* New York, NY: John Wiley & Sons, Inc.

De Luc, Jean-André. (1772). *Recherches sur les modifications de l'atmosphère.* Geneva: Royal Academy of Science of Paris.

Dictionaries, Editors of the American Heritage, ed. (2011). *American Heritage Dictionary of the English Language.* Fifth. Boston, MA: Houghton Mifflin Harcourt.

DuPont. (2014). *DuPont™ Tedlar® Polyvinyl Fluoride (PVF) Films.* Wilmington, DE: DuPont.

Edmunds, W. M. (2004). "Bath thermal waters: 400 years in the history of geochemistry and hydrogeology." *Geological Society, London, Special Publications* 225 (1): 193-199.

Ellis, A. J. (1957). "Chemical Equilibrium in Magmatic Gases." *American Journal of Science* 225: 416-431.

Etiope, G., Tsikouras, B., Kordella, S., Ifandi, E., Christodoulou, D. and Papatheodorou, G. (2013). "Methane flux and origin in the Othrys ophiolite hyperalkaline springs, Greece." *Chemical Geology* 161-174.

Etiope, G., Papatheodorou, G., Christodoulou, D. P., Ferentinos, G., Sokos, E. and Favali, P. (2006). "Methane and hydrogen sulfide seepage in the northwest Peloponnesus petroliferous basin (Greece): Origin and geohazard." *AAPG Bulletin* 90 (5): 701-713.

Eurofins Air Toxics, Inc. (2014). *Guide to Whole Air Sampling – Canisters and Bags.* Folsom, CA: Eurofins Air Toxics, Inc.

Fairchild, R.W., Hanson, R.L. and Davis, R.E. (1990). *Hydrology fo the Arbuckle Mountains Area, South-Central Oklahoma.* Norman, OK: Oklahoma Geologic Survey.

Fairley, T. (1881). "On the Blowing Wells near Northallerton." *Proceedings of the Yorkshire Geological & Polytechnic Society* VII: 482-494.

Farrell, P., Culling, D. Leifer, I. (2013). "Transcontinental methane measurements: Part 1. A mobile surface platform for source investigations." *Atmospheric Environment* 422-431.

Filho, J. S., Farias, M. S., Faccini, J. L., Lamy, C. A. and Su, J. (2009). High Speed Ultrasonic System to Measure Bubbles Velocities in a Horizontal Two-Phase Flow. *International Nuclear Atlantic Conference.* Rio de Janeiro,RJ, Brazil.

Fox, B. (1988). Secrets of the Source. *New Scientist*, 45-48.

Freeth, S. J. (1992). *The Lake Nyos gas disaster.* Braunschweig/Wiesbaden: Friedr.

Gallois, R. W. (2006). "The Geology of the Hot Springs at Bath Spa, Somerset." *Geoscience in south-west England* 11 (3): 168-173.

Gavrilović, D. (1967). "Intermitentni izvori u Jugoslaviji (Intermittent springs in Yugoslavia)." *Glasnik Srpskog Geografskog Drustva (Bulletin of the Serbian Geographical Society)* 13-36.

Geological Society of Pennsylvania. (1832). "Geology of Bradford County." *Minutes of the Geological Society of Pennsylvania.* 201.

Giggenbach, W. F. (1980). "Geothermal gas equilibria." *Geochimica et Cosmochimica Acta* 44 (12): 2021-2032.

Guo, L. and Riding, R. (2002). "Hot-spring travertine facies and sequences, Late Pleistocene, Rapolano Terme, Italy." *Sedimentology* 45: 163-180.

Hackley, K. C., Panno, S. V., Hwang, H. H. and Kelly, W. R. (2007). *Groundwater Quality of Springs and Wells of the Sinkhole Plain in Southwestern Illinois: Determination of the Dominant Sources of Nitrate.* Springfield, IL: Illinois Department of Natural Resources.

Hackley, K. C. and Panno, S. V. (2004). *Isotopic Analysis of Gas Seep from Little Calumet River.* Champaign, IL: Illinois State Geologic Survey.

Halihan, T., Mouri, S. and Pucket, J. (2009). *Evaluation of Fracture Properties of the Arbuckle-Simpson Aquifer.* Oklahoma City, OK: Oklahoma Water Resources Board.

Hall, C.M., Castro, M.C., Lohmann, K.C. and Ma, L. (2005). "Noble gases and stable isotopes in a shallow aquifer in southern Michigan: Implications for noble gas paleotemperature reconstructions for cool climates." *Geophysical Research Letters* 32 (L18404): 1-4. doi:10.1029/2005GL023582.

Hanson, B. R. and Schwankl, L. J. (1998). Water turbulence disrupts accuracy of some flow meters. *California Agriculture*.

Heaton, T. H. and Vogel, J. C. (1981). "Excess Air" in Groundwater. *Journal of Hydrology, 50*, 201-216.

Henry, W. (1803). "Experiments on the Quantity of Gases Absorbed by Water, at Different Temperatures, and under Different Pressures." *Philosophical Transactions of the Royal Society of London* (The Royal Society) 93: 29-42+274-276.

Herzberg, O. and Mazor, E. (1979). "Hydrological Applications of Noble Gases and Temperature Measurements in Underground Water Systems: Examples from Israel." *Journal of Hydrology* 41: 217-231.

Holocher, J., Peeters, F., Aeschbach-Hertig, W., Hofer, M., Brennwald, M., Kinzelbach, W. and Kipfer, R. (2002). Experimental investigations on the formation of excess air in quasi-saturated porous media. *Geochimica et Cosmochimica Acta, 66*(23), 4103-4117.

Hunt, A. (2015). U.S. Geological Survey Noble Gas Laboratory's Standard Operating Procedures for the Measurement. In *Book 5, Laboratory Analysis, Section A, Water Analysis, Chapter 11.* Denver, CO: USGS.

International Electrochemcial Commission. (2013). *IEC 60529-2013: DEGREES OF PROTECTION PROVIDED BY ENCLOSURES (IP CODE).* Geneva: IEC.

International Electrochemical Commission. (2007). *IEC 60664-1:2007 - Insulation coordination for equipment within low-voltage systems - Part 1: Principles, requirements and tests.* Geneva: IEC.

International Union of Pure and Applied Chemestry (IUPAC). (1997). *Compendium of Chemical Terminology (the "Gold Book").* 2nd. Edited by A D McNaught and A Wilkinson. Denmark: Blackwell Scientific Publications.

Jones, S. F., Evans, G. M. and Galvin, K. P. (1999). "Bubble nucleation from gas cavities; a review." *Advances in Colloid and Interface Science* 27-50.

Jung, M. and Aeschbach, W. (2018). A new software tool for the analysis of noble gas data sets from (ground)water. *Environmental Modeling Software, 103*, 120-130.

Kansou, K. and Bredeweg, B. (2014). "Hypothesis assessment with qualitative reasoning: Modelling the Fontestorbes fountain." *Ecological Informatics* 71-89.

Kauffman, E. G., Arthur, M. A., Howe, B. and Scholle, P. A. (1996). "Widespread venting of methane-rich fluids in Late Cretaceous (Campanian) submarine springs (Tepee Buttes), Western Interior seaway, U.S.A." *Geology* 799-802.

Keppel, M. N., Clarke, J. D. A., Halihan, T., Love, A. J. and Werner, A. D. (2011). "Mound springs in the arid Lake Eyre South region of South Australia: A new depositional tufa model and its controls." *Sedimentary Geology* 240: 55-70.

Kipfer, R., Aeschbach-Hertig, W., Peeters, F. and Stute, M. (2002). "Noble Gases in Lakes and Ground Waters." *Nobel Gases in Geochemistry and Cosmochemistry* (GeoScience World) 47 (1): 615-700. doi:10.2138/rmg.2002.47.14.

Klump, S., Cirpka, O. A., Surbeck, H. and Kipfer, R. (2008). Experimental and numerical studies on excess-air formation in quasi-saturated porous media. *Water Resources Research*, W05402.

Koch, U., Heinicke, J. and Voßberg, M. (2003). Hydrogeological effects of the latest Vogtland-NW Bohemian swarmquake period (August to December 2000). *Journal of Geodynamics, 35*, 107-123.

Krešić, N. (2007). *Hydrogeology and groundwater modeling* (Second ed.). Boca Raton, FL: CRC Press.

Kusakabe, M., Takeshi, O., Yutaka Yoshida, I., Satake, H., Ohizumi, T., Evans, W., Tanyileke, G. and Kling, G. (2008). "Evolution of CO2 in Lakes Monoun and Nyos, Cameroon, before and during controlled degassing." *Evolution of CO2 in Lakes Monoun and Nyos, Cameroon, before and during controlled degassing* 42: 93-118.

Lavenson, D., Kelkar, M., Daniel, A. V., Mohammad, A. B., Kouba, S. A. and Aichele, C. P. (2016). Gas evolution rates – A critical uncertainty in challenged gas-liquid separations. *Journal of Petroleum Science and Engineering*, 816-828.

LeConte, J. L. (1855). *Account of some volcanic springs in the desert of the Colorado in southern California.* New Haven, CT: Kline Geological Laboratory, Yale University.

Leeungculsatien, T. and Lucas, G. (2013). Measurement of velocity profiles in multiphase flow using a multi-electrode electromagnetic flow meter. *Flow MeasurementandInstrumentation*, 86-95.

Lewicki, J. L., Hilley, G. E., Dobeck, L., McLing, T. L., Kennedy, B. M., Bill, M. and Marino, B. D. V. (2013). "Geologic CO2 input into groundwater and the atmosphere, Soda Springs, ID, USA." *Chemical Geology* 339: 61-70.

Lim, H. H., Chang, K. A., Su, C. B. and Chen, C. Y. (2008). Bubble velocity, diameter, and void fraction measurements in a multiphase flow using fiber optic reflectometer. *Review of Scientific Instruments*.

Lowenstern, J. B., Bergfeld, D., Evans, W. C. and Hurwitz, S. (2012). "Generation and evolution of hydrothermal fluids at Yellowstone: Insights from the Heart Lake Geyser Basin." *Geochemistry, Geophysics, Geosystems* 13 (1). doi:10.1029/2011GC003835.

Lucchetti, G. and Gray, G. (1988). Water Reuse Systems: A Review of Principal Components. *The Progressive Fish-Culturist*, 1-6.

Madrzykowski, D. and Kerber, S. (2009). *Fire Fighting Tactics Under Wind Driven Conditions: Laboratory Experiments.* Gaithersburg, MD: National Institute of Standards and Technology.

Manning, A. H., Solomon, D. K. and Sheldon, A. L. (2003). Applications of a Total Dissolved Gas Pressure Probe in Ground Water Studies. *Ground Water, 41*(4), 440-448.

Mariner, R. H., Evans, W. C., Presser, T. S., and White, L. D. (2003). Excess nitrogen in selected thermal and mineral springs of the Cascade Range in northern California, Oregon, and Washington: sedimentary or volcanic in origin? *Journal of Volcanology and Geothermal Research*, 99-114.

Matsumoto, T., Han, L.-F., Jaklitsch, M., and Aggarwal, P. K. (2013). A Portable Membrane Contactor Sampler for Analysis of Noble Gases in Groundwater. *Ground Water, 51*(3), 461-468.

Mazor, E., and Wasserburg, G. J. (1965). "Helium, neon, argon, krypton and xenon in gas emanations from Yellowstone and Lassen volcanic National Parks." *Geochimica et Cosmochimica Acta* 29: 443-454.

McGrail, B P. (2001). "Inverse reactive transport simulator (INVERTS): an inverse model for contaminant transport with nonlinear adsorption and source terms." *Environmental Modelling & Software* 16 (8): 711-723. doi:https://doi.org/10.1016/S1364-8152(01)00035-4.

McLeod, H. C., Roy, J. W. and Smith, J. E. (2015). "Patterns of Entrapped Air Dissolution in a Two-Dimensional Pilot-Scale Synthetic Aquifer." *Groundwater* 53 (2): 271-281.

McLinn, E. L. and Stolzenburg, T. R. (2009). "Ebullition-Facilitated Transport of Manufactured Gas Plant Tar from Contaminated Sediment." *Environmental Toxicology and Chemistry* 28 (11): 2298-2306.

Meinzer, O. E. (1927). *Large Springs in the United States.* Water-Supply Paper 557, Washington, D.C.: Government Printing Office.

Merriam-Webster. (1950). *Webster's New International Dictionary of the English Language.* 2nd. Edited by William Allan Neilson. Springfield, MA: Merriam Company.

Mesonet. (2019). "Mesonet Long-Term Averages." doi:10.15763/dbs.mesonet.

Mesonet. (2019). "Ground Water Data." Board of Regents of the University of Oklahoma. http://www.mesonet.org/index.php/weather/groundwater/.

Mills, A. A. 2000. "Will-o'-the-wisp revisited." *Weather* 55: 239-241.

Mine Safety and Health Administration (MSHA). (2014). *Metal/Nonmetal Health Inspection Procedures Handbook.* Washington, D.C.: USGPO.

Mitchell, Rev. John. (1829). "Observations on Ignis Fatuus." *Journal of the Franklin Institute of the State of Pennsylvania* IV (2): 73-75.

Moorman, J. J. (1867). *Mineral Waters of the United States and Canada.* Baltimore, MD: Kelly & Piet.

Morgenstern, S. (1973). *The Princes Bride.* Edited by William Goldman. San Diego, CA: Harcourt Brace.

Musgrove, M., Opsahl, S.P., Mahler, B.J., Herrington, C., Sample, T.L. and Banta, J.R. (2016). "Source, variability, and transformation of nitrate in a regional karst aquifer: Edwards aquifer, central Texas." *Science of the Total Environment* 568: 457-469. http://dx.doi.org/10.1016/j.scitotenv.2016.05.201.

National Safety Council. (2012). *Fundamentals of Industrial Hygiene.* (B. A. Plog, & P. J. Quinlan, Eds.) Itasca, Il, USA: NSC Press.

Nestlé Waters North America Inc. (2016). *Bottled Water Quality Report.* Product Quality Report, Stamford, CT: Nestlé Waters North America Inc.

Nowamooz, A., Radilla, G. and Fourar, M. (2009). "Non-Darcian two-phase flow in a transparent replica." *Water Resources Research* 45. doi:10.1029/2008WR007315.

Ojima, M. and Podosek, F.A. (1983). *Noble Gas Geochemistry.* New York, NY: Cambridge University Press.

Oklahoma Water Resource Board. (2005-2018). "Water Level Measurements for Well 97451." *owrb.ok.gov.* https://www.owrb.ok.gov/wd/search_test/water_levels.php?siteid=97451.

Panno, S. V., Krapac, L. G., Weibel, C. P. and Bade, J. C. (1996). *Groundwater Contamination in Karst Terrain of Southwestern Illinois.* Champaign, IL: Illinois State Geologic Survey.

Panno, S. V., Hackley, K. C., Hwang, H. H. and Kelly, W. R. (2001). "Determination of the sources of nitrate contamination in karst springs using isotopic and chemical indicators." *Chemical Geology* 113-128.

Panno, S. V. (2001). *Report on Weldon Springs, IL.* Champaign, IL: Illinois State Geologic Survey.

Patoczka, J. and Wilson, D. (1984). Kinetics of the Desorption of Ammonia from Water by Diffused Aeration. *Separation Science and Technology*, 77-93.

Pedersen, K. (1999). "Evidence for a Hydrogen-driven, Intra-terrestrial Biosphere in Deep Granitic Rock Aquifers." *Subsurface Microbial Ecology.*

Peeters, F., Beyerle, U., Aeschbach-Hertig, W., Holocher, J., Brennwald, M.S. and Kipfer, R. (2002). "Improving noble gas based paleoclimate reconstruction and groundwater dating using 20Ne/22Ne ratios." *Geochimica et Cosmochimica Acta* 67 (4): 587-600.

Pollio, V. M. (1999). *De architectura.* Translated by Ingrid D. Rowland. Cambridge, England: Cambridge University Press.

Pradhan, S. (2010). Measurement of Bubble Velocity Vectors in Bubbly Air Water Multiphase Flow. *Doctoral thesis*. Huddersfield, West Yorkshire, England: University of Huddersfield.

Pruess, K., Oldenburg, C. and Moridis, G. (1999). *TOUGH2 USER'S GUIDE, VERSION 2.0.* User Guide, Berkeley, CA: Lawrence Berkeley National Laboratory.

Rich, K, Muehlenbachs, K., Uhrich, K. and Greenwood, G. (1995). "Carbon Isotope Characterization of Migrating Gas in the Heavy Oil Fields of Alberta, Canada." *International Heavy Oil Symposium.* Calgary, Alberta, Canada: Society of Petroleum Engineers.

Ricketts, J. W., Karlstrom, K. E., Priewisch, A., Crossey, L. J., Polyak, V. J. and Asmerom, Y. (2014). "Quaternary extension in the Rio Grande rift at elevated strain rates recorded in travertine deposits, central New Mexico." *Lithosphere* 6 (1): 3-16.

Ryan, M. C., MacQuarrie, K. T. B., Harman, J. and McLellan, J. (2000). "Field and modeling evidence for a "stagnant flow" zone in the upper meter of sandy phreatic aquifers." *Journal of Hydrology* 223-240.

Saiway, G., Mushrush, G. and Mose, D. (2006). Correlation Test Between Indoor Radon and Surficial Gamma Radiation in Northern Virginia. *Journal of Environmental Science and Health, 41*(Part A), 613-620.

Sander, R. (1999). *Compilation of Henry's Law Constants for Inorganic and Organic Species of Potential Importance in Environmental Chemistry.* Compilation, Mainz, Germany: Max-Planck Institute of Chemistry.

Scardina, P. (2004). "Effects of Dissolved Gas Supersaturation and Bubble Formation on Water Treatment Plant Performance." Blacksburg, VA: Virginia Polytechnic Institute and State University.

Scardina, P. and Edwards, M. (2006). "Fundamentals of Bubble Formation during Coagulation." *Journal of Environmental Engineering* 132: 575-585.

Schlosser, P., Stute, M., Sonntag, C. and Münnich, K. O. (1989). Tritiogenic 3He in shallow groundwater. *Earth and Planetary Science Letters, 94*, 245-256.

Schoell, M. (1988). "Multiple Origins of Methane in the Earth." *Chemical Geology* 1-10.

Schoell, M. (1980). "The hydrogen and carbon isotopic composition of methane from natural gases of various origins." *Geochemica et Cosmochimica Acta* 649-661.

Shipton, Z. K., Evans, J. P., Dockrill, D., Heath, J., Williams, A., Kirchner, D., and Kolesar, P. T. (2005). *Natural Leaking CO2-Charged Systems as Analogs for Failed Geologic Storage Reservoirs.* Vol. 2, chap. 4 in *Carbon Dioxide Capture for Storage in Deep Geologic Formations - Results from the CO2 Capture Project*, edited by Sally M. Benson, 699-712. Boston, MA: Elsevier.

Short, T. (1734). The Natural, Experimental, and Medicinal History of the Mineral Waters of Debyshire, Linconshire, and Yorkshire, Particularly those of Scarborough. London, England: Royal Society of London.

Sigurdsson, H., ed. (2000). *Encyclopedia of Volcanoes.* San Diego, CA: Academic Press.

Solomon, D. K., Cole, E. and Leising, J. F. (2011). Excess air during aquifer storage and recovery in an arid basin (Las Vegas Valley, USA). *Hydrogeology Journal*, 187-194.

Song, S., Schnorr, B. A. and Ramacciotti, F. C. (2014). Quantifying the Influence of Stack and Wind Effects on Vapor Intrusion. *Human and Ecological Risk Assessment*, 1345-1358.

Statista. (2016). *Sales of the leading bottled sparkling water brands of the United States in 2016.* New York, NY: Statista.

Stute, M. and Schlosser, P. (1993). Principles and Applications of the Noble Gas Paleothermometer. *Climate Change in Continental Isotopic Records, 78*, 89-100.

Stute, M., Forster, M., Frischkorn, H., Serejo, A., Clark, J. F., Schlosser, P. and Bonani, G. (1995). Cooling of Tropical Brazil (5˚C) During the Last Glacial Maximum. *Science, 269*(5222), 379-383.

Sugisaki, R. and Sugiura, T. (1986, November 10). Gas Anomalies at Three Mineral Springs and a Fumarole Before an Inland Earthquake, Central Japan. *Journal of Geophysical Research, 91*(B12), 12,296-12,304.

Sugisaki, R, and Tutomu, S. (1986). "Gas Anomalies at Three Mineral Springs and a Fumarole Before an Inland Earthquake, Central Japan." *Journal of Geophysical Research* 91 (B12): 12,296-12,304.

Sun, T., Hall, C.M. and Castro. M.C. (2010). "Statistical properties of groundwater noble gas paleoclimate models: Are they robust and unbiased estimators?" *Geochemistry Geophysics Geosystems* 11 (2): 1-18. doi:10.1029/2009GC002717.

Sun, T., Hall, C.M., Castro, M.C., Lohmann, K.C. and Goblet, R. (2008). "Excess air in the noble gas groundwater paleothermometer: A new model based on diffusion in the gas phase." *Geophysical Research Letters* 35 (L19401): 1-5. doi:10.1029/2008GL035018.

Swinea, J.T. (2008). *Thermal Controls on Springs in the Eastern Arbuckle-Simpson Aquifer (Dissertation).* Stillwater, OK: Oklahoma State University.

Tan, K.H. (2000). *Environmental Soil Science.* Edited by 2nd. New York, NY: M. Dekker.

Tanton, L. T. (1915). *The Relative Importance of Meteoric and Magmatic Waters in the Deposition of Certain Primary Ores.* Madison, WI: University of Wisconsin.

Taran, Y. A. (2005). A method for determination of the gas-water ratio in bubbling springs. *Geophysical Research Letters, 32*, L23403. doi:10.1029/2005GL024547

Thomas, J. M., Hudson, G. B., Stute, M. and Clark, J. F. (2002). Noble Gas Loss May Indicate Groundwater Flow Across Flow Barriers in Southern Nevada. *Environmental Geology, 43*, 568-579.

Thompson, G. G. and Withers, P. C. (2002). Aerial and aquatic respiration of the Australian desert goby, Chlamydogobius eremius. *Comparative Biochemistry and Physiology*, 871-879.

US Census Bureau. (2013). *Urban Areas in the United States and Puerto Rico (CPH-T-9) (2010 US Census Data).* Washington, DC: Government Printing Office. Retrieved from https://www.census.gov/data/tables/time-series/dec/cph-series/cph-t/cph-t-9.html

United States Department of the Interior Bureau of Reclamation. (2001). *Water Measurement Manual.* Washington, D.C.: US Government Printing Office.

Vroblesky, D. A. and Lorah, M. M. (1991). Prospecting for Zones of Contaminated Ground-Water Discharge to Steams Using Bottom-Sedement Gas Bubbles. *Ground Water, 29*(3), 333-340.

Wanninkhof, R., Asher, W. E., Ho, D. T., Sweeney, C. and McGillis, W. R. (2009). Advances in Quantifying Air-Sea Gas Exchange and Environmental Forcing. *Annual Review of Marine Science, 1*, 213-244. doi:10.1146/annurev.marine.010908.163742

Weast, R. C., ed. (1974). *Handbook of Chemestry and Physics.* 55th. Cleveland, OH: CRC Press.

Weiss, R. F. (1970). The Solubility of Nitrogen, Oxygen and Argon in Water and Seawater. *Deep-Sea Research, 17*, 721-735.

Weiss, R. F. (1971). Solubility of Helium and Neon in Water and Seawater. *Journal of Chemical and Engineering Data, 16*(2), 235-241.

Weiss, R. F. and Kyser, T. K. (1978). Solubility of Krypton in Water and Seawater. *Journal of Chemical and Engineering Data, 23*(1), 69-72.

White, D. E., Hem, J. D. and Waring, G. A. (1963). Chemical Composition of Sub-surface Waters. In M. Fleisher (Ed.), *Data of Geochemistry* (Sixth ed.). Washington D.C.: Government Printing Office.

Woodward, H. B. (1910). The Geology of Water-Supply. *Arnold's Geological Series*, 87-88.

Zeng, Z. and Grigg, R. (2006). A Criterion for Non-Darcy Flow in Porus Media. *Transport in Porous Media*, 57-69.

Żychowski, J. (2013). "Conditions favoring the occurrence of Ignis Fatuus phenomenon over a mass grave in Niepołomice (S Poland)." *The 3rd International Geography Symposium - GEOMED2013.* Cracow: Elsevier. 347-355.

APPENDIX

GLOSSARY OF BUBBLE RELATED TERMS

Boiling: Phase transition of a liquid to a gas (with the presence of bubbles) due to environmental conditions exceeding the *boiling point*. Specifically, the environmental temperature exceeds the liquid's *normal boiling point*. (Agnew-Halihan) See also Ebullate.

Boiling point: The conditions at which the vapor pressure of the liquid equals or exceeds the external environmental pressure surrounding the liquid. (American Industrial Hygiene Association 1998)

Bubble: Nearly spherical body of gas contained in a liquid. (Merriam-Webster 1950)

Churning: To stir or agitate violently (Merriam-Webster 1950). Mechanical turbulence of water in a spring or well due to upwelling. (Agnew-Halihan)

Ebullate/Ebullition: Phase transition of a dissolved gas coming out of solution (with the presence of bubbles) due to environmental conditions exceeding the *boiling point*. Specifically, the environmental pressure is less than the *saturation pressure* of the dissolved gas. (Agnew-Halihan) See also Boiling.

Evaporation: The process of phase transition of a liquid to a vapor (without the presence of bubbles). (Merriam-Webster 1950)

Excess Pressure (Supersaturation): The pressure of a dissolved gas in liquid beyond its *saturation pressure* at the *normal boiling point.* (Adapted from the American Heritage Dictionary of the English Language 2011)

Exsolution: A violent *ebullition* of a dissolved gas wherein the host liquid is displaced from its confining body i.e. a shaken up soda bottle. (Adapted from Sigurdsson 2000)

Fog: A condensed liquid aerosol suspended in air, typically with a droplet size sufficiently small as to be buoyant (visible). (American Industrial Hygiene Association 1998)

Gas: A substance that is in the *gaseous* state of matter above its *normal boiling point* (not visible). (Adapted from American Industrial Hygiene Association 1998 and Weast 1974)

Gaseous: A fluid (such as air) that has neither independent shape nor volume but tends to expand indefinitely, without reference to the substances *normal boiling point*, which may therefore be a *vapor* or a *gas*. (Adapted from Merriam-Webster 1950)

Mist: A mechanically generated liquid aerosol air in which the droplet size is typically sufficiently large as to cause settling (visible). (American Industrial Hygiene Association 1998)

Normal boiling point: The normal boiling point (also called the atmospheric boiling point) of a liquid is the special case in which the vapor pressure of the liquid equals or exceeds 101.325 kilopascals (kPa) (i.e. 1 atmosphere). (International Union of Pure and Applied Chemestry (IUPAC) 1997)

Roiling: Making turbid by stirring up the sediment or dregs of. (Merriam-Webster 1950)

Saturation Pressure: The pressure of a vapor which is in equilibrium with its liquid (100 relative humidity with respect to liquid water). (Merriam-Webster 1950)

Semi-Sparkling e.g. pétillant or frizzante: Having an *excess pressure* of CO^2 of not less than 1 bar and not more than 2.5 bar (250kPa) at 20 ºC (Council of the European Union 1999).

Sparkling e.g. Champagne: Having an *excess pressure* of CO_2 of not less than 3 bar (300kPa) at 20 ºC (Council of the European Union 1999).

Steam: Water in the *gaseous* state and at a temperature above its *normal boiling point*. (Adapted from Merriam-Webster 1950)

Vapor: A substance in the gaseous state below its normal boiling point (not visible), see evaporation. e.g. water vapor (Adapted from American Industrial Hygiene Association 1998, and Weast 1974)

Vapor Pressure: The vapor pressure of a liquid is the equilibrium pressure of a vapor above its liquid (or solid); that is, the pressure of the vapor resulting from evaporation of a liquid (or solid) above a sample of the liquid (or solid) in a closed container. (American Industrial Hygiene Association 1998)

Water Vapor: Water in vaporous form below its *normal boiling point*. (Merriam-Webster 1950)

VITA

Robert J. Agnew

Candidate for the Degree of

Doctor of Philosophy

Dissertation: MULTIPHASE GAS MECHANISMS IN GROUNDWATER

Major Field: Environmental Science

Biographical:

Education: Completed the requirements for the Doctor of Philosophy in Environmental Science at Oklahoma State University, Stillwater, Oklahoma in May, 2019.

Completed the requirements for the Master of Science in Industrial Hygiene at the University of Oklahoma Health Sciences Center, Oklahoma City, OK in 2002.

Completed the requirements for the Bachelor of Science in Engineering Technology – Fire Protection and Safety Technology at Oklahoma State University, Stillwater, OK in 1999.

Experience: Assistant Professor, Fire Protection & Safety Engineering Technology, Oklahoma State University, 2014-Present
Sr. Manager, Environmental, Health & Safety, Raytheon Company, 2002-2014
Industrial Hygienist, Liberty Mutual, 2000-2002
Environmental, Health & Safety Engineer, Seagate Company, 1999-2000

Professional Memberships: Certified Industrial Hygienist (CIH) 8603, American Board of Industrial Hygiene
Certified Safety Professional (CSP) 17684, Board of Certified Safety Professionals
Registered Environmental Manager (REM) 12032, National Registry of Environmental Professionals
American Industrial Hygiene Association (AIHA) National and Local Chapters